Re-Os geochronology and oil-source correlation of the Duvernay petroleum system, Western Canada sedimentary basin: Implications for the application of the Re-Os geochronometer to petroleum systems

Liu, Junjie[1]; Selby, David[1]; Obermajer, Mark[2]; Mort, Andy[2]

[1]Department of Earth Sciences, Durham University, Durham, DH1 3LE, UK

[2]Geological Survey of Canada, 33rd St. NW. Calgary, Alberta, T2L 2A7, Canada

Acknowledgements

This research was supported by funding from a Total research award and a China Scholarship Council grant to Junjie Liu, and the Total endowment fund to David Selby. We also thank the three AAPG reviewers and the AAPG Editor, Dr. Barry J. Katz, for their constructive comments, which improved this manuscript.

Abstract

The rhenium-osmium (Re-Os) geochronometer has been applied to many petroleum systems worldwide. However, it is debated if the Re-Os systematics in petroleum actually records the timing of oil generation. Here, we investigate the Re-Os isotope systematics of the Duvernay petroleum system in the Western Canada sedimentary basin, which has been shown to be a relatively simple petroleum system that is associated with oil generated during the Late Cretaceous - Early Eocene Laramide orogeny from a single source.

The organic geochemistry of the Duvernay oils (pristane/phytane ratios of ~1.5, smooth homohopane profile, $C_{29}>C_{27}>C_{28}$ regular sterane distribution, and predominance of diasteranes over regular steranes) strongly suggest the oil source to be that of Type I-II marine organic matter of the Late Devonian Duvernay Formation.

The asphaltene fraction Re-Os isotope data of the Duvernay oil yield an age of 66 ± 31 Ma, which is in excellent agreement with the timing of the main-stage hydrocarbon generation of the Duvernay Formation based on basin models. Further, the similarity between the $^{187}Os/^{188}Os$ compositions of the Duvernay Formation source rock (0.46 to 1.48) and the oil (0.55 to 1.06) at the time of oil generation supports the hypothesis that the $^{187}Os/^{188}Os$ composition of an oil is inherited from the source unit at the time of oil generation, and therefore shows no, or limited influence from interaction with basin fluids. This study supports that the Re-Os isotope systematics of an oil can yield the timing of oil generation, and be used to trace its source.

1. Introduction

Establishing an accurate and precise age of hydrocarbon generation is crucial for understanding the evolution of a petroleum system. Timing constraints for hydrocarbon generation can be achieved through many techniques, for example, basin modelling with paleotemperature and petroleum generation kinetics; or the timing of oil generation can be inferred by constraining the earliest migration of oil using radiometric dating ($^{40}Ar/^{39}Ar$) of fluid inclusions and diagenetic minerals, e.g., authigenic illite and K-feldspar (Eadington et

al., 1991; Kelly, 2002; Mark et al., 2005; Mark et al., 2010; Welte et al., 2012). Despite the contribution of these methods to the understanding of petroleum system evolution, they are limited by poorly constrained parameters (e.g., paleogeothermal gradient) or difficulties associated with sampling and analyzing (e.g., grain size versus purity of authigenic minerals for radiometric dating). During the past decade, the rhenium-osmium (Re-Os) chronometer has been demonstrated to be a promising radiometric tool to directly date petroleum samples and for oil-source correlation (Selby and Creaser, 2005b; Selby and Creaser, 2005a; Selby et al., 2007; Finlay et al., 2011; Finlay et al., 2012; Rooney et al., 2012; Lillis and Selby, 2013; Cumming et al., 2014; Ge et al., 2017).

Rhenium-Os analysis demonstrating chronologic information in petroleum systems was first shown by Selby et al. (2005), who derived a Re-Os date of 374.2 ± 8.6 Ma (MSWD = 11.7, Model 3) for bitumen formation in the Polaris Mississippi Valley Type deposit, Nunavut, Canada, which is in agreement with contemporaneous Pb-Zn mineralization dated at 366 ± 15 Ma (Rb-Sr sphalerite methodology). In addition, Re-Os data derived from highly biodegraded oil from the Oil Sand deposits of Alberta, Canada, give an age of 111.6 ± 5.3 Ma (MSWD = 2.2, Model 3) (Selby and Creaser, 2005a), which is in agreement with the basin model of Riediger et al. (2001). Consequently, the Re-Os date is taken to record the timing of oil generation and migration in the world's largest oil sand system. However, the Re-Os age for the oil sands is inconsistent with some other basin models proposed for this complex oil system, e.g. Higley et al. (2009), Berbesi et al. (2012), and a recent study on trap restoration

59 and the bitumen present in kimberlites (Tozer et al., 2014) which could relate to secondary
60 migration of oil in the Alberta basin.

61 Oil Re-Os dates (68 ± 13 Ma) from the UK Atlantic Margin (UKAM) petroleum system
62 (Finlay et al., 2011) also correspond to the age of petroleum generation determined through
63 basin modelling (Lamers and Carmichael, 1999) and K-feldspar cement $^{40}Ar/^{39}Ar$ dating
64 (Mark et al., 2005). A Re-Os study of oils from the Phosphoria petroleum system, Bighorn
65 basin, USA produced an age of 211 ± 21 Ma, corresponding to the start of petroleum
66 generation according to basin modelling rather than the re-migration of oil (during the
67 Laramide orogeny which starts from 80 - 70 Ma and ended until 55 - 35 Ma, although the
68 exact dates are in dispute; English and Stephen, 2004) or the deposition of the source rock
69 (during the Permian, ~270 Ma) (Lillis and Selby, 2013). Although the UKAM and
70 Phosphoria oils are variably biodegraded, the process has not appreciably disturbed the Re-
71 Os systematics from recording the timing of generation of oil. This is supported by the fact
72 that Re and Os in oil are hosted predominantly by the asphaltene fraction (Selby et al., 2007),
73 which is the most resistant phase to biodegradation (Wenger et al., 2001; Peters et al., 2005).
74 More recently, Re-Os bitumen data has provided insights into the temporal hydrocarbon
75 evolution in the Longmen Shan Thrust Belt, southwest China, i.e. the multiple oil generation
76 episodes (486 Ma and 172 - 162 Ma) and sources, and its relationship to tectonism, and
77 additionally discussed implications for future exploration of the adjacent petroliferous
78 Sichuan Basin (Ge et al., 2017). Furthermore, a study of the Green River petroleum system in
79 the Uinta basin, USA, demonstrated the capacity of the Re-Os chronometer to yield the

timing of oil generation (19 ± 14 Ma) in lacustrine petroleum systems in addition to marine petroleum systems (Cumming et al., 2014).

Unlike previous studies using multiple oil and/or bitumen samples to establish a Re-Os date, a study focusing on two oil families of the Gela oil field, southern Sicily, Italy, which are sourced from the Noto Formation (Upper Triassic, Rhaetian) and the Streppenosa Formation (Lower Jurassic, Hettangian), respectively, promotes the establishment of Re-Os dates using fractions of one single oil sample, in order to negate possible disadvantages of using multiple oil samples from a wide geographic region (Georgiev et al., 2016). The authors analysed the asphaltene and maltene fractions, which were separated using a series of solvents (*n*-pentane, *n*-hexane, *n*-heptane and *n*-decane). The best-fit lines of the Re-Os data for asphaltenes from one oil family and for maltenes from the other oil family yield reasonable oil generation ages for each family (27.5 ± 4.6 Ma and 200.0 ± 5.2 Ma, respectively). However, this approach of obtaining a Re-Os oil generation age from one single oil sample is potentially confined to oils with high asphaltene contents and Re and Os abundances. It also depends on the difference of asphaltenes and maltenes separated by different *n*-alkanes from the same oil to obtain a range in Re-Os isotopic compositions sufficient to obtain an isochron. As such, oils with low Re and Os abundances will be too analytically challenging to obtain precise data to distinguish these differences.

Hydrous pyrolysis experiments on organic-rich sedimentary rocks (Rooney et al., 2012; Cumming et al., 2014) have shown that during thermal maturation, Re and Os will be

transferred to the generated oil, although the majority of the Re and Os remains in the source rock. The $^{187}Re/^{188}Os$ values show no consistent relationship between the source rock and the generated oil, but the $^{187}Os/^{188}Os$ composition of a source rock is inherited by the generated oil (Selby et al., 2005; Finlay et al., 2011; Rooney et al., 2012; Cumming et al., 2014). The relationship between the $^{187}Os/^{188}Os$ composition of a source rock and the $^{187}Os/^{188}Os$ composition of the generated oil (at the time of generation) is employed in the aforementioned studies for oil-source correlation. For example, the attempt of identifying the source(s) for the Polaris bitumen through the Os isotope composition of a few Phanerozoic and Proterozoic potential source rocks led to the conclusion of the mix of several source rocks or a main source unit that was not sampled in the study for the studied bitumen. In addition, the coupling of Pt/Pd values with $^{187}Os/^{188}Os$ compositions has been employed as a viable inorganic oil-source correlation tool in recognizing the Lower Jurassic Gordondale Member as the predominant source of the Canadian oil sands (Finlay et al., 2012), which is supported by basin and migration modelling studies (Higley et al., 2009; Berbesi et al., 2012).

Although present studies show that biodegradation has little influence on the Re-Os systematics of asphaltene (Selby and Creaser, 2005a; Selby et al., 2005; Finlay et al., 2012; 2014), they can be vulnerable to other secondary alteration processes of petroleum. For example, disturbance of the Re-Os systematics has been shown for oils spatially associated with the main basin-bounding faults of the Viking Graben and East Shetland basin of the North Sea, United Kingdom (Finlay et al., 2010). Here, oils are suggested to have been contaminated by fault-charged mantle-fluids that contain Os with a non-radiogenic

$^{187}Os/^{188}Os$ composition. As a result, the Re-Os systematics of the oil fail to yield a generation age, but instead trace the crustal-scale fluid dynamics and migration. Such processes have also been demonstrated in the laboratory, where experiments have shown that Re and Os in aqueous phase can transfer into oil during oil-water contact under various conditions (Mahdaoui et al., 2015). Thermal cracking may also reset the Re–Os isotope systematics in petroleum and result in only the timing of thermal cracking and generation of dry gas and pyrobitumen being recorded (Lillis and Selby, 2013; Ge et al., 2016). Similarly, thermochemical sulphate reduction (TSR) of oil may also disturb or even reset the Re-Os systematics in oil. For example, the Re-Os data from oils affected by TSR in the Big Horn basin yield a Re-Os date of 9.24 ± 0.39 Ma, which is in agreement with the proposed end of TSR as a result of reservoir cooling due to the major uplift and erosion at ~10 Ma (Lillis and Selby, 2013).

The previous attempts and achievements of using Re-Os as petroleum generation geochronometer and oil-source tracer are often compromised by the lack of understanding, or intrinsic complex geological characteristics, of the petroleum systems. The source units of some petroleum systems are often debated or represent mixed sources. For example: 1) the Phosphoria system records a mixed oil generated from two separate members of the Permian Phosphoria Formation, i.e. Meade Peak Member (ca. 270 Ma) and Retort Member (ca. 265 Ma), which have an age difference of about 5 million years; 2) the Eocene Green River Formation (ca. 52 to 44 Ma) is over 3000 m (10000 ft) thick, within which many members are considered as possible oil sources (Anders et al., 1992; Ruble et al., 2001); 3) the

Canadian Oil Sands may have a mixed source, although the main contributor is highly debated (Riediger et al., 2001; Higley et al., 2009; Berbesi et al., 2012; Finlay et al., 2012; Adams et al., 2013). Inconsistent thermal maturation timings, multiple stages of oil generation and remigration are also often proposed by geological models. Both multiple sources and multiple stages, or prolonged oil generation, are likely to yield a large range of initial $^{187}Os/^{188}Os$ compositions of generated oil. Some oil samples are also altered (e.g., biodegradation, thermal cracking, and thermochemical sulphate reduction), for which the possibility and degree of disturbance to the oil Re-Os systematics has been discussed, but not yet fully understood. Further, the application of the $^{187}Os/^{188}Os$ composition as an oil-source correlation tool suffers from the lack of source rock Re-Os data in many cases. For example, the Green River Formation is over 3000 m (10000 ft) thick, but the shale samples for Re-Os dating were collected from three intervals with most of the samples spanning only 1 to 3 m (3 to 10 ft) (Cumming et al., 2014).

Here, as an examination of the usefulness of the application of the Re-Os chronometer in petroleum systems, we present the study on the simple and well-characterized Duvernay petroleum system of the Western Canada sedimentary basin (WCSB). The oil in this petroleum system is sourced from the Late Devonian Duvernay carbonaceous shale (Stoakes and Creaney, 1984; Li et al., 1998; Fowler et al., 2001). Oil generation from the Late Devonian Duvernay carbonaceous shale occurred during the Late Cretaceous to Eocene, associated with the Laramide orogeny (Deroo et al., 1977; Creaney and Allan, 1990). The generated oil migrated into the adjacent Leduc reef build-ups in the Rimbey-Meadowbrook

reef chain and Bashaw reef complex area, and then into the overlying Winterburn Group Nisku Formation (Creaney et al., 1994; Rostron, 1997). Biomarker analyses indicate that the Duvernay Formation is the only source of this petroleum system and that crude oil has experienced limited secondary alteration (Li et al., 1998; Fowler et al., 2001). We present Re-Os data from oil and source units, coupled with organic geochemistry, and discuss the geochronology and oil-source correlation of the Duvernay petroleum system and the implications for the application of the Re-Os geochronometer to petroleum systems.

2. Geological setting

The Duvernay petroleum system is located in south-central Alberta within the Western Canada sedimentary basin (Fig. 1). The Late Devonian Woodbend and Winterburn strata in the basin represent a thick and lithologically complex accumulation of shales and carbonates (Fig. 2). The two salient features of the Woodbend and Winterburn strata are the high quality source rocks and reservoirs they encompass, for example, the proliferous Duvernay Formation and the porous carbonates of the Leduc and Nisku Formations.

The Late Devonian Duvernay Formation of the Woodbend Group was deposited as marine basin-filling laminated carbonates and shales (Stoakes and Creaney, 1984; Switzer et al., 1994; Chow et al., 1995; Fowler et al., 2001; Fothergill, 2014). The Duvernay Formation correlates with the Muskwa Formation to the north, and the Horn River and Canol Formations in the Northwest Territories. The formation also overlies the platform carbonates of the Cooking Lake Formation and is in turn overlain by the basin-filling calcareous shales

of the Ireton Formation. The thickness varies depending on proximity to Devonian reef build-ups and is predominantly 20 - 60 m (60 to 200 ft) (Fig. 17, Switzer et al., 1994; Fothergill, 2014), but is up to 90 m (300 ft) within some carbonate embayments adjacent to the Killam Barrier reef-edge (Switzer et al., 1994; Fowler et al., 2001). The organic matter is concentrated in thin (typically a few mm) alternating laminae within the Duvernay Formation, which are separated by an organic-poor mudstone. Petrographically, the laminates of the Duvernay Formation contain abundant alganite macerals and some bituminite, often within an amorphous organic matrix, indicating that they represent periods of significant accumulation and preservation of oil-prone Type II marine organic matter (Fowler et al., 2001). This organic-poor mudstone becomes thinner (30 m (100 ft)) in the center of the basin (Switzer et al., 1994) to the west and reduces the separation between the two organic-rich intervals (Chow et al., 1995). The average TOC content ranges from 4 wt.% to 6 wt.%, although occasionally it is as high as 17 wt. % (Stoakes and Creaney, 1984; Chow et al., 1995; Higley et al., 2009; Dunn et al., 2012).

The numerous isolated Leduc reef build-ups (e.g., Rimbey-Leduc-Meadowbrook chain, Redwater, Bashaw) sit stratigraphically above the Cooking Lake and Beaverhill Lake Formations and partially interfinger with the Duvernay Formation (Fig. 1 - 2). The Leduc reefs are up to 275 m (900 ft) thick (Switzer et al., 1994; Chow et al., 1995; Rostron, 1997) and are highly porous and permeable (Amthor et al., 1994). A broad Leduc carbonate shelf also developed on the Cooking Lake Formation to the southeast of the basin. The Winterburn Nisku Formation is dominated by an extensive carbonate shelf in the East Shale basin to the

204 east of the Rimbey-Meadowbrook Leduc reef trend. Its thickness decreases from 60 m (200
205 ft) near the underlying Leduc reef trend to about 20 m (60 ft) in the east, with its lithology
206 changing stratigraphically from interbedded shale and limestone to relatively pure carbonates
207 (Switzer et al., 1994).

208 The hydrocarbon maturation of the majority of the Phanerozoic strata of the WCSB did not
209 occur until the Laramide orogeny (Late Cretaceous-Eocene) and was terminated by
210 subsequent uplift and erosion (Deroo et al., 1977; Creaney and Allan, 1990; Bustin, 1991). As
211 a result of the eastward propagation of crustal down-warping and foreland basin
212 development, deep burial and thermal maturation progressed from the foreland belt
213 northeastward across the plain. Present day isomaturity maps of Jurassic and younger source
214 rocks (Bustin, 1991) display a decrease in thermal maturity from the foredeep to the
215 shallower part of the basin in the northeast, where significant hydrocarbon generation
216 occurred until the Eocene. Also estimated by apatite fission track studies (Issler et al., 1999),
217 the peak paleo-temperature and inferred maximum burial depth is estimated from apatite
218 fission track dating to have occurred at ~ 60 Ma.

219 It is generally accepted that the Duvernay source rocks have generated large amounts of
220 hydrocarbons, with volume estimations ranging up to 100 million barrels (MMbbl) per square
221 mile (39 MMbbl per square kilometre; Jenden and Monnier, 1997). The generated oil
222 migrated extensively both laterally and stratigraphically within the basin, including in the
223 older Beaverhill Lake and Elk Point reservoirs. But migration of oils was largely confined to

224 the Cooking Lake-Leduc and Nisku Formations by the low permeability shales, dolomitic
225 carbonates and anhydrites of the Devonian Waterways Formation, Ireton Formation and
226 Wabamun Group (Fig. 3; Stoakes and Creaney, 1985; Creaney and Allan, 1990; Rostron,
227 1997) over most of central and northern Alberta. The generated oil migrated locally into the
228 Cooking Lake platform margins and Leduc reefs (Rimbey-Meadowbrook trend and Bashaw
229 Reefs), and the stratigraphically older Beaverhill Lake platform present in an updip position
230 due to the regional tilt of the strata (Fig. 31, Creaney and Allan, 1992; Creaney et al., 1994;
231 Fig. 5, Rostron, 1997. The Cooking Lake Formation also provided a migration pathway for
232 the isolated Leduc reef as a "leaky pipeline" dependent on the local presence or absence of
233 permeability barriers (Stoakes and Creaney, 1984). The Ireton shale serves as the seal to the
234 Duvernay petroleum system. However, due to the absence or the thin nature of the Ireton
235 shale in some places, oil also leaked into the overlying Nisku carbonates in the Bashaw area
236 (Rostron, 1997; Li et al., 1998). Geochemical studies (Creaney et al., 1994; Li et al., 1998;
237 Fowler et al., 2001) documented that the organic geochemical composition of the Duvernay
238 Formation extracts is quite similar to most of the crude oils found within the Leduc-Nisku
239 intervals along the Rimbey-Meadowbrook and Bashaw reef trends. In fact, geochemical oil-
240 source correlations have demonstrated that the Leduc and Nisku oils are almost all sourced
241 from the Duvernay Formation with probably only a very small contribution of the Nisku
242 source to the Nisku oils (Rostron, 1997; Li et al., 1998; Harris et al., 2003).

243 Gas chromatography and biomarker data show that there is no or limited alteration of the
244 Leduc and Nisku oils by biodegradation or water washing. Thermal cracking and

thermochemical sulphate reduction of crude oil occurred only in the foredeep (Evans et al., 1971; Rogers et al., 1974; Creaney and Allan, 1992; Marquez, 1994; Stasiuk, 1997; Fowler et al., 2001). The generated gas migrated up-dip and may have resulted in deasphalting, which is considered responsible for the high H_2S content of some of the stratigraphically-higher crude oil (Simpson, 1999; Fowler et al., 2001).

3. Sample preparation and analysis methodology

3.1 Oil samples

All oil samples analysed in this study were taken from the oil library of the Geological Survey of Canada - Calgary office (GSC-C). The selected oils are from both the Leduc and Nisku reservoirs in the area of the Rimbey-Meadowbrook Leduc reef trend and the Bashaw reef complex between Edmonton and Calgary (Fig. 1; Table 1). Prior to sampling, the archived oil was thoroughly mixed to remove any density separation of oil fractions that had occurred during storage.

The selected Duvernay oil samples typically have low asphaltene contents. Given that Re and Os are both predominantly present in the asphaltene fraction, and that the Re–Os isotopic composition of an asphaltene can be used as an approximation for that of the bulk oil (Selby et al., 2007), the asphaltene fractions were separated from the oils to permit more precise determinations of the Re and Os isotope compositions. The separation of asphaltene from the bulk oil follows the principles and steps outlined by Speight (2004) and Selby et al. (2007). For each gram of crude oil, 40 ml of *n*-heptane (or *n*-pentane) was added, and the mixture

was agitated on a rocker overnight (~ 20 h) at room temperature. Asphaltene is the insoluble fraction of oil in *n*-heptane (or *n*-pentane) and was isolated from the maltene-bearing *n*-heptane (or *n*-pentane) fraction by centrifuging at 3500 rpm for 15 minutes. Following the removal of the *n*-heptane (or *n*-pentane), the asphaltene was extracted using chloroform and dried at 60°C.

3.2 Source rock

In addition to the Duvernay oil asphaltene, the organic-rich Duvernay Formation was also analysed for its Re and Os abundances and Re-Os isotopic composition. The shale and carbonaceous shale samples of the Duvernay Formation were collected from the cores of wells 16-18-52-5W5, 14-29-48-6W5, 2-6-47-4W5 and 10-27-57-21W4 (Fig. 1; Table 2). The Re-Os data from these samples were compiled with previously published Re-Os data from the Duvernay Formation from wells 2-12-50-26W4, 8-35-31-25W4 and 1-28-36-3W5 (Selby et al., 2007; Finlay et al., 2012). The entire sample set covers a large geographical area of 300 × 150 km^2 (1866 × 93 sq mi). As a result, the sample set, with respect to hydrocarbon maturation, ranges from immature to highly mature with an average R_o from 0.5 % of 10-27-57-21W4 to 1.25 % of 2-6-47-4W5 and 1.45 % of 1-28-36-3W5 (Stasiuk and Fowler, 2002), and possesses highly variable TOC contents (from less than 1 wt.% to over 10 wt.%).

Depending on the thickness of the Duvernay Formation interval of each well, most samples were taken equally from each well at 0.5 m (1.6 ft; 16-18-52-5W5, ~1.5 m (4.9 ft)) and 2 m (7 ft; 14-29-48-6W5, ~8 m (26 ft); 2-6-47-4W5, ~20 m (60 ft)) or as equal as possible

depending on availability (10-27-57-21W4) in order to obtain a Re-Os data set that was representative of the entire Duvernay Formation organic-rich interval (Table 2). The collected core samples were cut and polished to remove any drilling marks and materials, and dried at 60˚C. Approximately 30 g of rock for each sample was crushed to a fine homogeneous powder using a Zr dish.

3.3 Organic geochemical analyses

All geochemical analyses were performed at the organic geochemistry laboratory of the Geological Survey of Canada - Calgary office. Pyrolysis of pulverized rock samples was carried out using Delsi Rock-Eval II and Rock-Eval 6 instruments (for measurement details see Espitalie et al., 1985; Behar et al., 2001). Biomarker analyses were performed on low- to high-maturity Duvernay sourced oil samples and source rock solvent extracts. Soluble organic matter was extracted from powdered rock samples of the Duvernay Formation for 24 hours using a chloroform:methanol (87:13) mixture. The extracts and crude oils were treated with approximately 40 volumes of *n*-pentane to precipitate the asphaltenes. The deasphalted extracts and oils were fractionated using open column chromatography. Saturates were recovered by eluting with pentane, aromatics by eluting with a 50:50 mixture of pentane-dichloromethane, and resins were recovered with methanol.

The gasoline range fractions (*i*-C_5-*n*-C_8) of the crude oils were analysed on a HP5890 Gas Chromatograph (50m HP-1 column, siloxane gum used as a fixed phase) connected to an OI Analytical 4460 Sample Concentrator. A small amount of the whole crude oil was mixed with

deactivated alumina and transferred to the Sample Concentrator. The temperature was initially held at 30 °C for 10 minutes, then increased at a rate of 1 °C/min to 45 °C and held for 25 minutes. The eluting hydrocarbons were detected using a flame ionization detector.

Saturate fractions were analysed using a Varian 3700 FID gas chromatograph equipped with a 30m DB-1 column. The temperature was programmed from 60 °C to 300 °C at a rate of 6 °C/min and then held for 30 min at 300 °C. Gas chromatography-mass spectrometry (GCMS) was performed on a VG 7070 mass spectrometer with a gas chromatograph attached directly to the ion source (30 m (100 ft) DB-5 fused silica column used for GC separation). The temperature was initially held at 100 °C for 2 min and then programmed at 40 °C/min to 180 °C and at 4 °C/min to 320 °C. After reaching 320 °C, the temperature was held for 15 min. The mass spectrometer was operated with a 70 eV ionization voltage, 100 mA filament emission current, and interface temperature of 280 °C.

3.4 Re-Os analyses

The measurement of asphaltene and shale Re and Os abundances, and Re and Os isotopic compositions were undertaken at Durham University in the Laboratory for Source Rock and Sulphide Geochronology and Geochemistry (a member of the Durham Geochemistry Centre) by isotope dilution - negative thermal ionization mass spectrometry (ID-NTIMS). The chemical processing of samples to isolate and purify Re and Os and the measurement by NTIMS follow previously published protocols (Selby and Creaser, 2001; Selby and Creaser, 2003; Selby, 2007; Rooney et al., 2011; Cumming et al., 2014). In brief, a known amount of

shale (~0.1 to 1 g) and asphaltene (~0.15 g), together with a known amount of mixed spike containing ^{185}Re and ^{190}Os, was digested by a Cr^{VI}-H_2SO_4 solution for shale and inverse *aqua-regia* (2:1 16 N HNO_3 and 12 N HCl, 9 ml) for asphaltene in carius tubes at 220˚C for 48 hrs. For some of the samples, the amount of asphaltene digested is limited by the amount of asphaltene obtained from the oil. The Os was extracted from the digested samples using chloroform, and then back-extracted from the chloroform using 9N HBr, before being purified by micro-distillation. Following the Os extraction, for shale samples, a 1 ml aliquot of the Cr^{VI}-H_2SO_4 solution was evaporated to dryness, and the Re fraction was isolated using sodium hydroxide-acetone solvent extraction, before being further purified by anion chromatography. For the asphaltene samples, the *aqua-regia* was evaporated to dryness and the Re fraction purified by anion chromatography. The purified Re and Os were loaded onto Ni and Pt filaments, respectively (Selby et al., 2007). Isotopic measurements were conducted using negative thermal ionization mass spectrometry (Creaser et al., 1991; Völkening et al., 1991) on a Thermo Scientific TRITON mass spectrometer via ion-counting, using a secondary electron multiplier in peak-hopping mode for Os, and static Faraday collection for Re. In-house solution standards are 0.1611 ± 0.0004 (1SD, n = 126) for DROsS (Durham Romil Osmium Solution) and 0.5989 ± 0.0019 (1SD, n = 116) for Re Standard solution, which are in agreement with those previously reported (Luguet et al., 2008; Nowell et al., 2008; Cumming et al., 2012).

The measured difference in $^{185}Re/^{187}Re$ values for the Re standard solution and the accepted $^{185}Re/^{187}Re$ value (0.5974; Gramlich et al., 1973) is used for mass fractionation correction of

346 the Re sample data. All Re and Os data are oxide and blank corrected. The total procedural
347 blanks of inverse *aqua-regia* are ~ 1.6 pg Re and 0.04 ~ 0.1 pg Os, with an average
348 $^{187}Os/^{188}Os$ of 0.24 ± 0.06 (n = 3). The total procedural blanks of Cr^{VI}-H_2SO_4 digested
349 samples are ~12 pg Re and 0.02 ~ 0.05 pg Os, with average $^{187}Os/^{188}Os$ of 0.22 ± 0.06 (n =
350 4). All uncertainties are determined by error propagation of uncertainties in Re and Os mass
351 spectrometer measurements, weighing, blank abundances and isotopic compositions, spike
352 calibrations, and the reproducibility of standard Re and Os isotopic values. The Re-Os data
353 are regressed using *Isoplot* (V. 4.15; Ludwig, 2012) with the ^{187}Re decay constant value of
354 1.666×10^{-11} yr^{-1} (Smoliar et al., 1996). This decay constant is also used for the calculation of
355 the $^{187}Os/^{188}Os$ values of the shales at the time of deposition and oil generation, and the
356 $^{187}Os/^{188}Os$ values of the asphaltene at oil generation.

357 ## 4. Results

358 ### 4.1 Asphaltene Re-Os data

359 The asphaltene contents and Re-Os data of asphaltene fractions of this study, and one analysis
360 reported by Selby et al. (2007), are shown in Table 3. The asphaltene abundance of the
361 sampled Duvernay oils is between 0.23 and 14.10 %. Coupled with low asphaltene contents
362 are low Re and Os abundances of the asphaltene fractions, which range from 0.01 to 3.78 ppb
363 Re, 0.6 to 41.2 ppt Os, and 0.2 to 14.9 ppt ^{192}Os, respectively. Oil samples possessing
364 asphaltene abundances up to ~4 % show a positive correlation between asphaltene abundance
365 and both Re and ^{192}Os (representing unradiogenic common Os) abundances (Fig. 4).

366 However, this relationship does not hold for the remaining oil samples that possess higher
367 asphaltene content (6 – 8% and ~15%) (Fig. 4). Though, in general, oil samples possessing
368 higher asphaltene contents have higher Re and ^{192}Os abundances (Fig. 4). The low Re and Os
369 abundances, coupled with the limited asphaltene obtained for Re-Os analyses, make precise
370 measurements very challenging. The majority of the samples possess blank corrections
371 between 0.3 – 3.3 % for Re and 1 - 10 % for Os (L02221 to L02155), although a few samples
372 (e.g., L01810) have significant Re and Os corrections (40% Re and 50% Os). The samples
373 with such large blank corrections also possess large uncertainties. Samples with uncertainty
374 greater than 55% for $^{187}Re/^{188}Os$ and 30% for $^{187}Os/^{188}Os$ are excluded when determining a
375 Re-Os age and are not further discussed. The $^{187}Re/^{188}Os$ and $^{187}Os/^{188}Os$ values of the
376 asphaltene used for isochron construction range between ~67 and 642, and 0.78 and 1.62,
377 respectively (Table 3). Together with the sample of Selby et al. (2007), the Re-Os data yield a
378 Model 3 date (a model assuming variable initial $^{187}Os/^{188}Os$ values for samples) of 66 ± 31
379 Ma (n = 14, MSWD = 6.7, initial $^{187}Os/^{188}Os$ = 0.77 ± 0.20; Fig. 5-6).

380 ## 4.2 Re-Os data for organic-rich intervals of the Duvernay Formation

381 The Re and Os abundances and isotope data for the Duvernay source rock analysed from four
382 wells of this study, plus those of previous studies (Selby et al., 2007; Finlay et al., 2012) are
383 reported in Table 2. The Re and Os abundances for the Duvernay source range between 0.3
384 and 68 ppb Re, and 29 and 1965 ppt Os. The more Re- and Os- (^{192}Os) enriched sectors of the
385 Duvernay source rock broadly correlate with intervals possessing higher TOC abundances

386 (Fig. 7). The $^{187}Re/^{188}Os$ and $^{187}Os/^{188}Os$ ratios range from ~26 to 229 and 0.49 to 1.74,
387 respectively.

388 We have calculated the $^{187}Os/^{188}Os$ composition of the Duvernay Formation at the time of
389 deposition (initial $^{187}Os/^{188}Os$ (Os_i)), a value that is equal to the $^{187}Os/^{188}Os$ composition of
390 the contemporaneous seawater (Cohen et al., 1999). The biostratigraphy of the Duvernay
391 Formation shows mainly the occurrence of *Palmatolepis punctata* and *Palmatolepis hassi*
392 (Ziegler and Sandberg, 1990; McLean and Klapper, 1998; Whalen et al., 2000), which
393 constrains the deposition age to be between 376.5 and 380.5 Ma based on the Geologic
394 Timescale 2016 (Ogg et al., 2016). The Os_i values for the shale samples are calculated at
395 378.5 Ma. The Os_i values range between 0.28 and 0.38, with a Tukey's Biweight mean
396 (which weighs the points according to their scatter from the iteratively-determined mean) of
397 0.33 ± 0.01 (n = 33; Table 2; Fig. 7).

398 ## 4.3 Organic geochemistry of crude oil and rock samples

399 The Leduc-Nisku oils, although typically not altered by biodegradation or water-washing,
400 show a wide range of thermal maturities, often resulting in variable geochemical
401 characteristics, and have been classified into three main subgroups that include low-, normal-
402 and high-maturity oils (Fig. 8). These hydrocarbons, however, represent a continuum that can
403 be easily documented by examples of crude oils having maturities intermediate between the
404 three subgroups. The following overview pertains mostly to the saturated hydrocarbon
405 fractions of the three oil sub-types resulting from differences in thermal maturity (although

similar compositional variations have also been observed in the aromatic fraction by Li et al., 1998). Main compositional characteristics of the organic extracts and a brief oil-source correlation summary are also included.

The least mature Duvernay sourced oils are found in the Leduc and Nisku reservoirs in central eastern Alberta, to the south of the Bashaw Reef Complex. These oils are characterized by low saturate/aromatic ratio, relatively high amounts of NSO compounds, and relatively high sulphur content (1-1.5%). Gasoline range chromatograms show high *n*-heptane and methylcyclohexane peaks (*n*-C_7>MCH), with toluene often in relatively high abundance compared to most other oils sourced from Devonian units. Saturate fraction gas chromatograms display smooth distribution of n-alkanes with slight odd carbon number preference of *n*-C_{15} – *n*-C_{19} members, high abundance of acyclic isoprenoids relative to n-alkanes, low pristane/phytane ratio (~0.80), and evident biomarkers.

Biomarker distributions show a smooth homohopane (C_{31}–C_{35}) profile, gammacerane present in moderate abundance, low amounts of rearranged hopanes (i.e. low Ts/Tm (abbreviations are annotated in Table 4)) and tricyclic and tetracyclic terpanes relative to 17α(H)-hopane, C_{24} tetracyclic terpane in similar abundance to the two C_{26} tricyclic terpane isomers, relatively low abundances of diasteranes and short-chain steranes relative to regular steranes, and a C_{27}-C_{29} sterane abundance of C_{29}>C_{27}>>C_{28}.

The majority of the oil pools along the Rimbey-Meadowbrook trend contain normal-maturity Duvernay Formation sourced oils. Compared to low maturity oils, these oils have higher

saturate/aromatic ratios, lower amounts of NSO compounds and lower sulphur content.

Gasoline range and saturate fraction gas chromatograms are generally similar in both subgroups, with notably lower abundance of acyclic isoprenoids relative to *n*-alkanes and some biomarker peaks in more mature oils.

Furthermore, normal maturity oils contain higher amounts of rearranged hopanes (hence higher Ts/Tm), tricyclic and tetracyclic terpanes compared to the hopanes, C_{24} tetracyclic terpane slightly greater than C_{26} tricyclic terpanes, very low abundance of gammacerane, higher abundances of diasteranes and short-chain steranes, and similar carbon number distributions for C_{27}-C_{29} regular steranes.

The high maturity Duvernay sourced oils and condensates tend to be those from the deeper, westerly pools with higher API gravities, typically occurring in the southern half of the province. Compared with other Duvernay sourced oils, they have higher saturate/aromatic ratios and lower amounts of NSO compounds. Although these oil can still be correlated to oils from the other two subgroups by gasoline range and saturate fraction gas chromatography data (though maturation parameters indicate higher maturity and *n*-alkane profiles shows more bias towards lower molecular weight homologues), they are quite easily distinguished based on the lack of or very low abundance of biomarkers such as hopanes and steranes. The visible peaks in the m/z 191 and m/z 217 chromatograms are typically tricyclic terpanes, Ts and C_{29} Ts, low molecular weight steranes, high diasteranes and secosteranes with an extremely low abundance of regular steranes.

446 The analysis of the available Duvernay Formation Rock-Eval and TOC data reveals this unit
447 contains on average 4% of organic carbon with the maximum of up to 18%, enough to be
448 considered as petroleum source rock (Fig. 9). In thermally unaltered and low maturity
449 samples hydrogen index values are up to 700 indicating presence of Type I-II organic matter
450 (Fig. 10). Although the extract yields are commonly above 100 mg total extract/g TOC, and
451 greater than 200 mg in about 1/3 of the samples, the hydrocarbon yields typically range from
452 20 to 80, with few above 100 mg HC/g TOC (Fig. 11), which overall is indicative of good
453 source rock potential. The extract data show no evidence of staining, as the proportions of
454 hydrocarbons in extracts are normally less than 50% (Fig. 11)

455 The gas chromatograms of the extracts typically show *n*-alkane distributions dominated by
456 shorter-chain homologues (n-C_{15} – n-C_{20}) (Fig. 12). Amounts of acyclic isoprenoids relative
457 to *n*-alkanes are high in low maturity samples and decrease with increasing level of thermal
458 maturity. Pristane/phytane ratios generally fall within 1-2 range. Saturate biomarker
459 signatures of mature extracts show relatively high amounts of rearranged hopanes and
460 steranes with no homohopane prominence, low tricyclic terpanes, Ts/Tm ratios greater than
461 1.0 and high diasteranes. The geochemical character of the Duvernay Formation extracts is
462 different compared with other Devonian units in Alberta that show petroleum source potential
463 (Creaney et al., 1994).

464 Correlation of biomarker data indicates that organic geochemical composition of the
465 thermally mature Duvernay Formation solvent extracts is very similar to that of the normal

466 maturity crude oils found within the Leduc-Nisku intervals along the Rimbey-Meadowbrook
467 and Bashaw reef trends (Fig. 13). Both extracts and oils have higher concentrations of *n*-C_{17}
468 and *n*-C_{18} relative to pristane and phytane, and average Pr/Ph ratios typical of suboxic
469 depositional conditions (average of 1.66 and 1.38 for extracts and oils, respectively), show
470 predominace of Ts over Tm, a smooth homohopane distributions without C_{34} or C_{35}
471 prominence, relatively high amounts of rearranged steranes and common C_{29}>C_{27}>C_{28}
472 regular sterane profile (Fig. 14). Their overall similarity and genetic relationship are further
473 supported by regional geology and stratigraphic data. As noted previously (Stoakes and
474 Creaney, 1984 and 1985; Li et al., 1998), the Duvernay strata is the only prolific source rock
475 interval that occurs in close stratigraphic proximity to the Leduc reefs to account for the large
476 volume of oil found in the Leduc reservoirs and, therefore, is considered as the main source
477 of these oils.

478 # 5 Discussion

479 ## 5.1 Petroleum Re-Os geochronology

480 The burial history of the Albertan part of the Western Canada sedimentary basin has been
481 constructed with isopach maps of the stratigraphic formations (Deroo et al., 1977; Higley et
482 al., 2005) and basin modelling based on oil generation kinetic parameters (Higley et al., 2009;
483 Berbesi et al., 2012), which indicate that the Duvernay Formation started to generate oil at the
484 onset of the Laramide orogeny, i.e., around 80 Ma. According to the most recent basin models
485 (Higley et al., 2009; Berbesi et al., 2012), the majority of the oil generation occurred between

~70 and ~58 Ma, with a significant kerogen transformation ratio (>50%) of the Duvernay Formation being reached by ~65 Ma, and cessation of oil generation by ~50 Ma due to basin uplift.

The Re-Os oil date (66 ± 31 Ma, n = 14, MSWD = 6.7; Fig. 5) obtained from the asphaltene fraction Re-Os data, although possessing a large uncertainty, is in good agreement with the timing of peak oil generation indicated by geological modelling. It is clear that the Re-Os oil date does not in any way reflect the age of the Duvernay Formation which is the source of Duvernay oil (this study; Deroo et al., 1977; Creaney et al., 1994; Li et al., 1998), i.e. early Late Devonian (Frasnian; this study; Switzer et al., 1994).

The Re-Os date is derived from a Model 3 *Isoplot* solution (Ludwig, 2012), which means that the scatter about the best-fit line (the isochron), as represented by the MSWD (mean square weighted deviation) value, is due to a combination of the calculated uncertainties for the $^{187}Re/^{188}Os$ and $^{187}Os/^{188}Os$ values and the error correlation, rho, plus an unknown but normally distributed variation in the initial $^{187}Os/^{188}Os$ (Os_i) values. The uncertainty in the Re-Os date spans the entire duration of oil generation; however, it is not to say that the uncertainty of the Re-Os oil age will necessarily be indicative of the duration of oil generation. The MSWD value (6.7) being >1 for the best-fit line suggests that the scatter about the best-fit line is controlled by geological factors rather than purely analytical uncertainties (Ludwig, 2012). The ~25% uncertainty in the calculated initial Os_i composition (0.77 ± 0.20, Fig. 5; 0.55 to 1.06, Fig. 6-7, Table 3) suggests that the primary factor causing the degree of scatter about the best-fit of the Re-Os data is the variation in the Os_i

507 composition of the oil sample set. The geological cause of the variation in the Os_i
508 composition of the Duvernay oil is discussed below (Section 5.2). Although the Re-Os date
509 for the generation of Duvernay sourced oil is not as precise or detailed as the basin modeling,
510 Re-Os oil geochronology works directly on oil samples and can provide comparison and
511 validation of the oil generation dating by traditional geological tools in a fast and economic
512 way.

513 ## 5.2 $^{187}Os/^{188}Os$ composition oil-source fingerprinting

514 Previous research has proposed that at the time of oil generation, an oil inherits the
515 $^{187}Os/^{188}Os$ composition of the source rock (Selby et al., 2005; Selby and Creaser, 2005;
516 Finlay et al., 2011; Finlay et al., 2012; Rooney et al., 2012; Cumming et al., 2014). Compared
517 to the previous attempts to apply the $^{187}Os/^{188}Os$ composition of oil and source rock as an
518 absolute fingerprinting tool, the Duvernay petroleum system benefits from its single source
519 and simple thermal maturation history. Here we have also obtained source rock Re-Os data
520 for the entire stratigraphic interval of the Duvernay Formation over a large geographical area,
521 to reflect the source rock Re-Os systematics as completely as possible.

522 Although not sampled for shale geochronology, for which an intensive sampling strategy
523 should be adopted to minimize the time span of samples and limit any possible variability in
524 the initial $^{187}Os/^{188}Os$ value, the Duvernay Formation source rock $^{187}Re/^{188}Os$ and $^{187}Os/^{188}Os$
525 data do display a positive correlation and yield Late Devonian ages (well 10-27-57-21W4, 10
526 samples over 55 m (180 ft), Re-Os data yield 371 ± 22 Ma, initial $^{187}Os/^{188}Os = 0.33 \pm 0.03$,

MWSD = 66; well 16-18-52-5W5, 4 samples over 1.5 m (5 ft), Re-Os data yield 372 ± 13 Ma, initial $^{187}Os/^{188}Os$ = 0.33 ± 0.02, MWSD = 0.06; well 14-29-48-6W5, 5 samples over 6 m (20 ft), Re-Os data yield 377 ± 62 Ma, initial $^{187}Os/^{188}Os$ = 0.33 ± 0.14, MWSD = 84; well 2-6-47-4W5, 11 samples over 20 m (60 ft), Re-Os data yield 360 ± 15 Ma, initial $^{187}Os/^{188}Os$ = 0.38 ± 0.03, MWSD = 33; Fig. 15). Further, given that the samples analysed are considered broadly the same geological age (Fig. 15A-D), we also present a calculated Re-Os date from all 33 samples. The Re-Os data for the entire sample set yield 373.9 ± 9.4 Ma, with an initial $^{187}Os/^{188}Os$ = 0.34 ± 0.02 (MWSD = 82; Fig. 15E). The uncertainties of the ages are due to the variation in the Os_i compositions (Table 2, Fig. 7), which range from 0.28 to 0.38, and the limited spread in the $^{187}Re/^{188}Os$ values (≤160 $^{187}Re/^{188}Os$ units; Table 2 and Fig. 15). Although the Re-Os dates are imprecise, they are nominally in agreement with the Late Devonian biostratigraphic age constraints for the Duvernay Formation.

To evaluate the relationship between the oil Os_i (Fig. 5-6) composition and that of the source rock at the time of oil generation, the Duvernay source rock $^{187}Os/^{188}Os$ compositions at 66 Ma (Os_g) are calculated from the present day Re-Os data of shale samples. The Duvernay Formation Os_g values range between 0.46 and 1.48 (n = 33 from 7 wells), and yield a Tukey's Biweight mean of 0.83 ± 0.01 (Tables 2; Fig. 7). The oil Os_i defined by the Re-Os isochron is 0.77 ± 0.20 (Fig. 5). The range of the individual oil Os_i values is between 0.55 and 1.06 (Fig. 6). Seventy-nine percent (26 of the 33 samples) of the shale Os_g values are indistinguishable from the individual oil Os_i values (Fig. 7). The evidence from organic geochemistry of the Duvernay petroleum system indicates that the Duvernay Formation is the principal source of

548 the Duvernay oils. As such, the similarity of the oil Os_i and Duvernay Formation Os_g
549 compositions supports the research hypothesis that the oil Os_i is inherited from the source at
550 the time of oil generation, and therefore oil Os_i and source Os_g values can be used as an oil-
551 source correlation tool.

552 An oil-source correlation based on Os isotopic compositions is supported by the comparison
553 of Duvernay petroleum system oil Os_i and shale Os_g values with the Os_g values of other oil-
554 prone strata of the WCSB. As most of the oil-prone Phanerozoic strata of the WCSB
555 underwent hydrocarbon maturation during the Laramide orogeny (Bustin, 1991; Higley et al.,
556 2009), the Os_g values of these strata with available Re-Os data are also calculated at 66 Ma
557 (Table 5; Fig. 16). However, in contrast to the Duvernay petroleum system oil Os_i and shale
558 Os_g values, the Os_g values of the other oil-prone strata of the WCSB are distinctly more
559 radiogenic (e.g., the Gordondale Member of the Early Jurassic Fernie Formation (Selby et al.,
560 2007; Finlay et al., 2012) has Os_g values are between 0.99 and 4.06, with an arithmetic
561 average and median of 2.04 and 1.51; the Devonian-Mississippian Exshaw Formation
562 (Creaser et al., 2002; Selby and Creaser, 2003; Finlay et al., 2012) has Os_g values between
563 1.35 and 4.96 with an arithmetic average and median of 2.22 and 1.93; the Middle Devonian
564 Keg River Formation (Miller, 2004) laminates of La Crete basin have Os_g values between
565 1.34 and 4.25, with an arithmetic average and median of 1.97 and 1.64). The exceptions to
566 the latter are the Os_g values of the kukersites of the Ordovician Yeoman Formation, Williston
567 basin (Miller, 2004), which are between 0.46 and 5.36, with an arithmetic average and
568 median of 1.21 and 0.84. The Ordovician kukersites Os_g values are only slightly more

569 radiogenic than the Duvernay petroleum system oil Os_i and shale Os_g values, however, it can
570 be spatially (eastern Montana - western North Dakota and southern Saskatchewan versus
571 south-central Alberta) excluded as the source of the Duvernay oils (Creaney et al., 1994). The
572 Os_i and Os_g data, coupled with the organic geochemistry, support the Duvernay Formation as
573 the key source unit of the Duvernay oils, and eliminate the other oil-prone Phanerozoic strata
574 of the WCSB as sources of the Duvernay petroleum system.
575 Although we show a strong similarity between the Os_i and Os_g values for the Duvernay oils
576 and Formation, we observe that the Os_g values in the cores studied here and the oil Os_i values
577 show some heterogeneity (Fig. 5-7). If we consider each core separately, the average Os_g
578 values are nominally skewed either positively or negatively to the overall average of the Os_g
579 values (0.83 ± 0.01; Fig. 15; Table 2). For example, the Tukey's Biweight mean of Os_g values
580 for core 10-27-57-21W4 is 0.72 ± 0.12, for core 12-6-47-4W5 it is 0.90 ± 0.17, for core 14-
581 29-48-6W5 it is 0.96 ± 0.07, and for core 16-18-52-5W5 the arithmetic average is 0.66 ± 0.22
582 (2 SD; weighted by assigned errors only as Tukey's Biweight mean is not suitable for its
583 small sample set).
584 The change in the $^{187}Os/^{188}Os$ composition from the time of source rock deposition to the
585 time of oil generation is dependent on the duration between deposition and hydrocarbon
586 maturation, and the Re abundance in the source rock. Variability in the Re abundance
587 stratigraphically, plus the variations in local seawater $^{187}Os/^{188}Os$ values inherited by the
588 organic-rich rock, such as that shown by the Duvernay Formation (Table 2), results in
589 heterogeneous $^{187}Os/^{188}Os$ values with ^{187}Re decay (Table 2; Fig. 7 and 15).

As such, if the heterogeneous Os_g is inherited by the generated oils then our data propose that the oil generated from different geographical sections of the same source interval could lead to reservoired oils possessing variable Os_i. The primary migration and expulsion of oil within and from a source rock, which is often broadly contemporaneous with or occurs shortly after oil generation, could result in the homogenization of the $^{187}Os/^{188}Os$ values of oil. Although, the extent of homogenization should depend on many factors (e.g. permeability of source rock and carrier beds). In the case of the Duvernay Formation, the oils generated could possess a range in Os_i from 0.46 to 1.48, which is similar to what is observed in this study with the Duvernay oil Os_i values, ranging from ~0.55 to 1.06 (Table 2 - 3; Fig. 5-7). The variability in the Os_i values makes it analytically challenging to obtain a precise isochron (66 ± 31 Ma). The determined Os_i by the isochron (0.77 ± 0.20) demonstrates the variability in the Os_i values. As such, if we select the samples with the most similar Os_i (e.g., L00864, L00873, L02196, L02220 and L02221), a Re-Os date of 56 ± 18 Ma is obtained, with an Os_i of 0.74 ± 0.10 and MSWD of 0.33. The Re-Os date still coincides with the timing of hydrocarbon maturation associated with the Laramide orogeny, but is almost 50% more precise.

5.3 Oil Re-Os systematics: effect of oil-water contact

Although we propose that the Re and Os in oil are inherited from a source rock, based on the similarity of the Os_i values of the asphaltene fractions and the Os_g values of the Duvernay Formation shales, an experimental study has suggested that Re and Os in oil can also be derived from contact with formation water (Mahdaoui et al., 2015). The outcome of this

611 experimental work has recently been questioned (Wu et al., 2016), particularly based on the
612 several orders of magnitude higher Re and Os concentrations applied in the experiment
613 (0.001 to 100 μg/g Re and 1 or 10 ng/g Os) compared with the known low Re and Os
614 concentrations of basin fluids (typically 4 pg/g Re and 70 fg/g Os; Mahdaoui et al. (2015)) in
615 most oil-bearing sedimentary basins. Nevertheless, we consider here if the oil Re-Os
616 systematics may have been affected by or originated from the basin fluids in the Leduc reef
617 trend and Nisku Formation. There are very limited Re and Os data for basin fluids available
618 at present and if we also use the typical formation water Re and Os abundances of 4 pg/g and
619 70 fg/g, respectively (Mahdaoui et al., 2015), approximately 2 to 40 g of such water contains
620 equivalent Re and Os in 1 gram of Duvernay oil (Table 3). Such oil-water contact ratios are
621 highly probable in a petroleum system (Magoon and Dow, 1991). As such, based on the
622 experiments of Mahdaoui et al. (2015), the Re-Os systematics of the low Re- and Os-bearing
623 Duvernay oils could have been easily influenced by oil-basin fluid interaction and reflect the
624 Os isotopic composition of the basin fluid. However, comparing the $^{87}Sr/^{86}Sr$ values of Late
625 Devonian seawater of 0.7080 - 0.7084 (Burke et al., 1982) with the $^{87}Sr/^{86}Sr$ values of
626 calcites and dolomite cements (0.7088 - 0.7108) of the Leduc Rimbey-Meadowbrook reef
627 trend (Stasiuk, 1997), and that of the current brines of Nisku Formation (0.70998-0.71206)
628 and Leduc Formation (0.70872 - 0.70981) (Connolly et al., 1990), it is suggested that the
629 basin fluids could have interacted with the radiogenic crystalline basement and/or Proterozoic
630 - Lower Cambrian clastics (Mountjoy et al., 1999). As such, the $^{187}Os/^{188}Os$ compositions of
631 the basin fluids should be radiogenic, considering the high $^{187}Os/^{188}Os$ initial values of these

strata (Kendall et al., 2009) and the long duration between the depositional age and the timing of oil generation. For example, the Neoproterozoic Old Fort Point Formation has an initial $^{187}Os/^{188}Os$ value of ~ 0.62 at deposition of 608 Ma (Kendall et al., 2004), which will have radiogenically evolved to $^{187}Os/^{188}Os$ values >3 at 66 Ma (Table 5). Further, considering a lower end member $^{187}Re/^{188}Os$ value of 100 for the crystalline basement and/or Proterozoic - Lower Cambrian strata and an initial $^{187}Os/^{188}Os$ composition of 0.5, the decay of ^{187}Re over ≥450 million years will yield a $^{187}Os/^{188}Os$ value > 1.25 at the time that the Duvernay Formation underwent thermal maturation. The deep-originated basinal fluids interacted with old strata and therefore should have very radiogenic $^{187}Os/^{188}Os$ compositions. The minimum estimate of the $^{187}Os/^{188}Os$ composition of the basinal fluid is more radiogenic than the present day (0.78 – 1.62) and initial (0.77 ± 0.20) values of the Duvernay oil . As a result, we propose that the predominant Re and Os budget and the isotope systematics of the Duvernay oil represent that inherited from the Duvernay Formation source rocks during thermal maturation, and not Re and Os sequestered from basin fluids. And therefore the Os_i values are inherited at the time of oil generation, and are ultimately linked to the source rock rather than formation fluids.

Conclusions

Despite the uncertainty of Re-Os asphaltene isotopic data of the Duvernay oils, which is a direct result of the low Re and Os abundance, the limited range in the $^{187}Re/^{188}Os$ values, and the variation in the Os_i values of the asphaltene, the Re-Os age derived from asphaltene

652 fractions agrees well with the widely accepted burial and hydrocarbon maturation models that
653 indicate that hydrocarbon generation occurred long after source rock deposition during the
654 Laramide orogeny. Further, the similarity between the oil Os_i values and the Duvernay
655 Formation Os_g values, and their difference to other oil-prone strata of the WCSB, coupled
656 with the evidence from organic geochemistry, confirms the Duvernay Formation as the
657 source and the ability of the $^{187}Os/^{188}Os$ composition as an oil-source correlation tool.
658 Moreover, the Duvernay-sourced oils Re-Os systematics are not considered to have been
659 significantly affected by basin fluids, indicating that the majority of Re-Os systematics in the
660 oil (asphaltene fraction) is inherited from its source.

661 We suggest that one of the major factors controlling the precision of a Re-Os date for oil
662 relates to the variation in Os_i values inherited by an oil from its source at the time of oil
663 generation, which is independent of the radiogenic evolution of the $^{187}Os/^{188}Os$ composition
664 in the source rock. For example, the relative homogeneous $^{187}Os/^{188}Os$ of Duvernay
665 Formation at the time of deposition (Os_i = ~0.33) evolved with time to a heterogeneous
666 $^{187}Os/^{188}Os$ composition due to the variable Re abundance in the source unit. The
667 heterogeneous $^{187}Os/^{188}Os$ composition of the Duvernay Formation was inherited by the
668 generated oil. Our data suggests that basin wide thorough homogenization of the Os isotopic
669 composition did not occur during migration.

670 The agreement of the Re-Os asphaltene date, coupled with the similarity of the Os_i and Os_g
671 values of the asphaltene and Duvernay Formation, respectively, of the relatively simple

672 Duvernay petroleum system of Western Canada sedimentary basin with basin models and
673 organic geochemistry confirms the potential ability of the Re-Os oil (asphaltene fraction)
674 systematics to record the timing of hydrocarbon generation, and to serve as an effective oil-
675 source correlation tool.
676

References

Adams, J., S. Larter, B. Bennett, H. Huang, J. Westrich, and C. van Kruisdijk, 2013, The dynamic interplay of oil mixing, charge timing, and biodegradation in forming the Alberta oil sands: Insights from geologic modeling and biogeochemistry, *in* F. J. Hein, D. Leckie, S. Larter, and J. R. Suter, eds., Heavy-oil and oil-sand petroleum systems in Alberta and beyond: AAPG Studies in Geology 64, p. 23–102. DOI:10.1306/13371578St643552.

Aitken, J.D., and D. K. Norris, 2014, WEBLEX Canada, Lexicon of Canadian geologic names on-line, <http://weblex.nrcan.gc.ca/weblexnet4/weblex_e.aspx>, accessed November 2017.

Amthor, J. E., E. W. Mountjoy, and H. G. Machel, 1994, Regional-scale porosity and permeability variations in Upper Devonian Leduc buildups: Implications for reservoir development and prediction in carbonates: AAPG Bulletin, v. 78, no. 10, p. 1541-1558. doi:10.1306/a25ff215-171b-11d7-8645000102c1865d

Anders, D. E., J. G. Palacas, and R. C. Johnson, 1992, Thermal maturity of rocks and 944 hydrocarbon deposits, Uinta Basin, Utah, *in* Thomas D. Fouch, Vito F. Nuccio, Thomas C. Chidsey, Jr., eds., Hydrocarbon and mineral resources of the Uinta Basin, Utah and Colorado: Utah Geological Association Guidebook, no. 20, p. 53-74.

Behar, F., V. Beaumont, H. L. Penteado, and B. De, 2001, Rock-Eval 6 Technology: Performances and developments. Revue de l' Français du Pétrole, v. 56, no. 2, p. 111-134. DOI: 10.2516/ogst:2001013

698 Berbesi, L. A., R. di Primio, Z. Anka, B. Horsfield, and D. K. Higley, 2012, Source rock
699 contributions to the Lower Cretaceous heavy oil accumulations in Alberta: A basin
700 modeling study: AAPG Bulletin, v. 96, no. 7, p. 1211-1234. DOI:
701 10.1306/11141111064
702 Burke, W., R. Denison, E. Hetherington, R. Koepnick, H. Nelson, and J. Otto, 1982,
703 Variation of seawater $^{87}Sr/^{86}Sr$ throughout Phanerozoic time: Geology, v. 10, no. 10, p.
704 516-519. DOI: 10.1130/0091-7613(1982)10<516:VOSSTP>2.0.CO;2
705 Bustin, R., 1991, Organic maturity in the Western Canada sedimentary basin: International
706 Journal of Coal Geology, v. 19, no. 1, p. 319-358. DOI: 10.1016/0166-
707 5162(91)90026-F
708 Chow, N., J. Wendte, and L. D. Stasiuk, 1995, Productivity versus preservation controls on
709 two organic-rich carbonate facies in the Devonian of Alberta: Sedimentological and
710 organic petrological evidence: Bulletin of Canadian Petroleum Geology, v. 43, no. 4,
711 p. 433-460.
712 Cohen, A. S., A. L. Coe, J. M. Bartlett, and C. J. Hawkesworth, 1999, Precise Re–Os ages of
713 organic-rich mudrocks and the Os isotope composition of Jurassic seawater: Earth and
714 Planetary Science Letters, v. 167, no. 3-4, p. 159-173. DOI: 10.1016/s0012-
715 821x(99)00026-6
716 Connolly, C. A., L. M. Walter, H. Baadsgaard, and F. J. Longstaffe, 1990, Origin and
717 evolution of formation waters, Alberta basin, Western Canada sedimentary basin. II.
718 Isotope systematics and water mixing: Applied Geochemistry, v. 5, no. 4, p. 397-413.

719 DOI: 10.1016/0883-2927(90)90017-Y
720 Creaney, S., and J. Allan, 1990, Hydrocarbon generation and migration in the Western
721 Canada sedimentary basin: Geological Society, London, Special Publications, v. 50,
722 no. 1, p. 189-202. DOI: 10.1144/GSL.SP.1990.050.01.9
723 Creaney, S., 1992, Petroleum Systems in the foreland basin of Western Canada, *in* R.
724 Macqueen and D. Leckie, eds., Foreland basins and fold belts: AAPG Memoir 55, p.
725 279-308.
726 Creaney, S., J. Allan, K. Cole, M. Fowler, P. Brooks, K. Osadetz, R. Macqueen, L. Snowdon,
727 and C. Riediger, 1994, Petroleum generation and migration in the Western Canada
728 sedimentary basin, *in* G. D. Mossop and I. Shetson, eds., Geological Atlas of the
729 Western Canada sedimentary basin, p. 455-468.
730 Creaser, R. A., P. Sannigrahi, T. Chacko, and D. Selby, 2002, Further evaluation of the Re-Os
731 geochronometer in organic-rich sedimentary rocks: A test of hydrocarbon maturation
732 effects in the Exshaw Formation, Western Canada sedimentary basin: Geochimica et
733 Cosmochimica Acta, v. 66, no. 19, p. 3441-3452. DOI: 10.1016/S0016-
734 7037(02)00939-0
735 Cumming, V. M., D. Selby, and P. G. Lillis, 2012, Re–Os geochronology of the lacustrine
736 Green River Formation: Insights into direct depositional dating of lacustrine
737 successions, Re–Os systematics and paleocontinental weathering: Earth and Planetary
738 Science Letters, v. 359-360, p. 194-205. DOI: 10.1016/j.epsl.2012.10.012
739 Cumming, V. M., D. Selby, P. G. Lillis, and M. D. Lewan, 2014, Re–Os geochronology and

740 Os isotope fingerprinting of petroleum sourced from a Type I lacustrine kerogen:
741 Insights from the natural Green River petroleum system in the Uinta basin and
742 hydrous pyrolysis experiments: Geochimica et Cosmochimica Acta, v. 138, p. 32-56.
743 DOI: 10.1016/j.gca.2014.04.016
744 Deroo, G., T. G. Powell, B. Tissot, and R. G. McCrossan, 1977, The origin and migration of
745 petroleum in the Western Canadian sedimentary basin, Alberta - A geochemical and
746 thermal maturation study: Geological Survey of Canada Bulletin 262, 136 p.
747 Dunn, L., G. Schmidt, K. Hammermaster, M. Brown, R. Bernard, E. Wen, R. Befus, and S.
748 Gardiner, 2012, The Duvernay Formation (Devonian): Sedimentology and reservoir
749 characterization of a shale gas/liquids play in Alberta, Canada (abs.), *in* Proceedings
750 Canadian Society of Petroleum Geologists: Annual Convention, Calgary.
751 Eadington, P., P. Hamilton, and G. Bai, 1991, Fluid history analysis - A new concept for
752 prospect evaluation: Australian Petroleum Exploration Association Journal, v. 31, no.
753 1, p. 282-294.
754 Energy Resources Conservation Board, Calgary, Alberta, Canada, 2009, Table of
755 formations, Alberta, <ags.aer.ca/document/Table-of-Formations.pdf>, accessed
756 December 12, 2014.
757 English, J. M. and S. T. Johnston, 2004, The Laramide orogeny: what were the driving
758 forces?. International Geology Review, v. 46, no. 9, p. 833-838. DOI: 10.2747/0020-
759 6814.46.9.833.
760 Espitalie, J., G. Deroo, and F. Marquis, 1985, Rock Eval Pyrolysis and Its Applications.

761 Preprint; Institut Francais du Petrole, Geologie No. 27299, 72 p. English translation
762 of, La pyrolyse Rock-Eval et ses applications, Premiere, Deuxieme et Troisieme
763 Parties, in Revue de l'Institut Francais du Petrole, v. 40, p. 563-579 and 755-784; v.
764 41, p. 73-89. DOI: 10.2516/ogst:1985035
765 Evans, C. R., M. A. Rogers, and N. J. L. Bailey, 1971, Evolution and alteration of petroleum
766 in Western Canada: Chemical Geology, v. 8, no. 3, p. 147-170.
767 Finlay, A. J., D. Selby, M. J. Osborne, and D. Finucane, 2010, Fault-charged mantle-fluid
768 contamination of United Kingdom North Sea oils: Insights from Re-Os isotopes:
769 Geology, v. 38, no. 11, p. 979-982. DOI: 10.1130/G31201.1
770 Finlay, A. J., D. Selby, and M. J. Osborne, 2011, Re-Os geochronology and fingerprinting of
771 United Kingdom Atlantic Margin oil: Temporal implications for regional petroleum
772 systems: Geology, v. 39, no. 5, p. 475-478. DOI: 10.1130/G31781.1
773 Finlay, A. J., D. Selby, and M. J. Osborne, 2012, Petroleum source rock identification of
774 United Kingdom Atlantic Margin oil fields and the Western Canadian Oil Sands using
775 Platinum, Palladium, Osmium and Rhenium: Implications for global petroleum
776 systems: Earth and Planetary Science Letters, v. 313-314, p. 95-104. DOI:
777 10.1016/j.epsl.2011.11.003
778 Fothergill, P. A., D. Boskovic, P. Murphy, M. Mukati, and N. Schoellkopf, 2014, Regional
779 Modelling of the Late Devonian Duvernay Formation, Western Alberta, Canada:
780 Unconventional Resources Technology Conference (URTEC), p. 95-102..
781 Fowler, M. G., L. D. Stasiuk, M. Hearn, and M. Obermajer, 2001, Devonian hydrocarbon

782 source rocks and their derived oils in the Western Canada sedimentary basin: Bulletin
783 of Canadian Petroleum Geology, v. 49, no. 1, p. 117-148. DOI: 10.2113/49.1.117
784 Fowler, M. G., M. Obermajer, and L. D. Stasiuk, 2003, Rock-Eval/TOC data for Devonian
785 potential source rocks, Western Canada sedimentary basin: Geological Survey of
786 Canada Open File 1579. DOI: dx.doi.org/10.4095/214440
787 Ge, X., C. Shen, D. Selby, D. Deng, and L. Mei, 2016, Apatite fission-track and Re-Os
788 geochronology of the Xuefeng uplift, China: Temporal implications for dry gas
789 associated hydrocarbon systems: Geology, v. 44, no. 6, p. 491-494. DOI:
790 10.1130/G37666.1
791 Ge, X., C. Shen, D. Selby, J. Wang, L. Ma, X. Ruan, S. Hu, L. Mei, 2017, Petroleum
792 generation timing and source in the Northern Longmen Shan Thrust Belt, Southwest
793 China: Implications for multiple oil generation episodes and sources: AAPG Bulletin,
794 in press. DOI: 10.1306/07111716230 17125
795 Georgiev, S. V., H. J. Stein, J. L. Hannah, R. Galimberti, M. Nali, G. Yang, and A.
796 Zimmerman, 2016, Re-Os dating of maltenes and asphaltenes within single samples
797 of crude oil: Geochimica et Cosmochimica Acta, v. 179, p. 53-75. DOI:
798 10.1016/j.gca.2016.01.016
799 Gramlich, J. W., T. J. Murphy, E. L. Garner, and W. R. Shields, 1973, Absolute isotopic
800 abundance ratio and atomic weight of a reference sample of rhenium: Journal of
801 Research of the National Bureau of Standards – A. Physics and Chemistry, v. 77A, no.
802 6, p. 691–698. DOI: 10.6028/jres.077A.040

803 Harris, S. A., M. J. Whiticar, and M. G. Fowler, 2003, Classification of Duvernay sourced
804 oils from central and southern Alberta using Compound Specific Isotope Correlation
805 (CSIC): Bulletin of Canadian Petroleum Geology, v. 51, no. 2, p. 99-125. DOI:
806 10.2113/51.2.99
807 Higley, D. K., M. Henry, L. N. R. Roberts, and D. W. Steinshouer, 2005, 1-D/3-D geologic
808 model of the Western Canada sedimentary basin: The Mountain Geologist, v. 42, no.
809 2, p. 53-66.
810 Higley, D. K., M. D. Lewan, L. N. R. Roberts, and M. Henry, 2009, Timing and petroleum
811 sources for the Lower Cretaceous Mannville Group oil sands of northern Alberta
812 based on 4-D modeling: AAPG Bulletin, v. 93, no. 2, p. 203-230. DOI:
813 10.1306/09150808060
814 Issler, D. R., S. D. Willett, C. Beaumont, R. A. Donelick, and A. M. Grist, 1999,
815 Paleotemperature history of two transects across the Western Canada sedimentary
816 basin: Constraints from apatite fission track analysis: Bulletin of Canadian Petroleum
817 Geology, v. 47, no. 4, p. 475-486.
818 Jenden, P. D., and F. Monnier, 1997, Regional variations in initial petroleum potential of the
819 Upper Devonian Duvernay and Muskwa formations, Central Alberta (abs.): Canadian
820 Society of Petroleum Geologists - SEPM Joint Convention: Program with Abstracts,
821 Calgary, p. 146
822 Kelley, S., 2002, K-Ar and Ar-Ar dating: Reviews in Mineralogy and Geochemistry, v. 47,
823 no. 1, p. 785-818. DOI: 10.2138/rmg.2002.47.17

824 Kendall, B. S., R. A. Creaser, G. M. Ross, and D. Selby, 2004, Constraints on the timing of
825 Marinoan “Snowball Earth” glaciation by ^{187}Re–^{187}Os dating of a Neoproterozoic,
826 post-glacial black shale in Western Canada: Earth and Planetary Science Letters, v.
827 222, no. 3-4, p. 729-740. DOI: 10.1016/j.epsl.2004.04.004
828 Kendall, B., R. A. Creaser, and D. Selby, 2009, ^{187}Re-^{187}Os geochronology of Precambrian
829 organic-rich sedimentary rocks: Geological Society, London, Special Publications, v.
830 326, no. 1, p. 85-107. DOI: 10.1144/SP326.5
831 Lamers, E., and S. M. M. Carmichael, 1999, The Paleocene deepwater sandstone play West
832 of Shetland: Geological Society of London, Petroleum Geology Conference series, v.
833 5, p. 645-659. DOI: 10.1144/0050645
834 Li, M., H. Yao, M. G. Fowler, and L. D. Stasiuk, 1998, Geochemical constraints on models
835 for secondary petroleum migration along the Upper Devonian Rimbey-Meadowbrook
836 reef trend in central Alberta, Canada: Organic Geochemistry, v. 29, no. 1-3, p. 163-
837 182. DOI: 10.1016/s0146-6380(98)00094-1
838 Lillis, P. G., and D. Selby, 2013, Evaluation of the rhenium–osmium geochronometer in the
839 Phosphoria petroleum system, Bighorn basin of Wyoming and Montana, USA:
840 Geochimica et Cosmochimica Acta, v. 118, p. 312-330. DOI:
841 10.1016/j.gca.2013.04.021
842 Ludwig, K., 2012, User’s manual for Isoplot version 3.75-4.15: a geochronological toolkit for
843 Microsoft: Excel Berkley Geochronological Center Special Publication, no. 5.
844 Luguet, A., G. M. Nowell and D. G. Pearson, 2008, $^{184}Os/^{188}Os$ and $^{186}Os/^{188}Os$

measurements by negative thermal ionisation mass spectrometry (N-TIMS): Effects of interfering element and mass fractionation corrections on data accuracy and precision. Chemical Geology, v. 248, no. 3, p. 342–362. DOI: 10.1016/j.chemgeo.2007.10.013

Magoon, L., and W. Dow, 1991, The petroleum system - From source to trap: AAPG Bulletin, v. 75, no.3, p. 627.

Mahdaoui, F., R. Michels, L. Reisberg, M. Pujol, and Y. Poirier, 2015, Behavior of Re and Os during contact between an aqueous solution and oil: Consequences for the application of the Re–Os geochronometer to petroleum: Geochimica et Cosmochimica Acta, v. 158, p. 1-21. DOI: 10.1016/j.gca.2015.02.009

Mark, D. F., J. Parnell, S. P. Kelley, M. Lee, S. C. Sherlock, and A. Carr, 2005, Dating of multistage fluid flow in sandstones: Science, v. 309, no. 5743, p. 2048-2051. DOI: 10.1126/science.1116034

Mark, D. F., J. Parnell, S. P. Kelley, M. R. Lee, and S. C. Sherlock, 2010, $^{40}Ar/^{39}Ar$ dating of oil generation and migration at complex continental margins: Geology, v. 38, no. 1, p. 75-78. DOI: 10.1130/G30237.1

Marquez, X., 1994, Reservoir geology of Upper Devonian Leduc buildups, deep Alberta basin: Ph. D. Dissertation, McGill University, Montreal, Canada, 285 p.

McLean, R. A., and G. Klapper, 1998, Biostratigraphy of Frasnian (Upper Devonian) strata in western Canada, based on conodonts and rugose corals: Bulletin of Canadian Petroleum Geology, v. 46, no. 4, p. 515-563.

866 Miller, C. A., 2004, Re-Os dating of algal laminites reduction-enrichment of metals in the
867 sedimentary environment and evidence for new geoporphyrins: Master of Science
868 Dissertation, University of Saskatchewan, Saskatoon, Canada, 153 p. DOI:
869 handle:10388/etd-06242011-085331
870 Mountjoy, E. W., H. G. Machel, D. Green, J. Duggan, and A. E. Williams-Jones, 1999,
871 Devonian matrix dolomites and deep burial carbonate cements: a comparison between
872 the Rimbey-Meadowbrook reef trend and the deep basin of west-central Alberta:
873 Bulletin of Canadian Petroleum Geology, v. 47, no. 4, p. 487-509.
874 Nowell, G., A. Luguet, D. Pearson, and M. Horstwood, 2008, Precise and accurate
875 $^{186}Os/^{188}Os$ and $^{187}Os/^{188}Os$ measurements by multi-collector plasma ionisation mass
876 spectrometry (MC-ICP-MS) part I: Solution analyses: Chemical Geology, v. 248, no.
877 3, p. 363-393. DOI: 10.1016/j.chemgeo.2007.10.020
878 Ogg, J., G. Ogg, and F. M. Gradstein, 2016, A Concise Geologic Time Scale 2016,
879 Amsterdam, Elsevier, 242 p.
880 Peters, K. E., C. C. Walters, and J. M. Moldowan, 2005, The biomarker guide, volume 2 -
881 Biomarkers and isotopes in petroleum exploration and earth history: Cambridge:
882 Cambridge University Press, v. 475, 634 p.
883 Powell, T.G., 1978, An assessment of the hydrocarbon source rock potential of the Canadian
884 Arctic Islands. Geological Survey of Canada, Paper 78-12, 82 p.
885 Riediger, C. L., S. Ness, M. Fowler, and N. T. Akpulat, 2001, Timing of oil generation and
886 migration, northeastern British Columbia and southern Alberta - Significance for

887 understanding the development of the eastern Alberta tar sands deposits (abs.): AAPG
888 Annual Convention Official Program, v. 10, p. A168.
889 Rogers, M. A., J. McAlary, and N. Bailey, 1974, Significance of reservoir bitumens to
890 thermal-maturation studies, Western Canada basin: AAPG Bulletin, v. 58, no. 9, p.
891 1806-1824.
892 Rooney, A. D., D. M. Chew, and D. Selby, 2011, Re–Os geochronology of the
893 Neoproterozoic–Cambrian Dalradian Supergroup of Scotland and Ireland:
894 Implications for Neoproterozoic stratigraphy, glaciations and Re–Os systematics:
895 Precambrian Research, v. 185, no. 3-4, p. 202-214. DOI:
896 10.1016/j.precamres.2011.01.009
897 Rooney, A. D., D. Selby, M. D. Lewan, P. G. Lillis, and J. P. Houzay, 2012, Evaluating Re–
898 Os systematics in organic-rich sedimentary rocks in response to petroleum generation
899 using hydrous pyrolysis experiments: Geochimica et Cosmochimica Acta, v. 77, p.
900 275-291. DOI: 10.1016/j.gca.2011.11.006
901 Rostron, B. J., 1997, Fluid flow, hydrochemistry and petroleum entrapment in Devonian reef
902 complexes, south-central Alberta, Canada. *in* S.G. Pemberton and D.P. James eds.,
903 Petroleum Geology of the Cretaceous Mannville Group: Canadian Society of
904 Petroleum Geologists Memoir 18, Calgary, p. 169-190.
905 Ruble, T. E., M. Lewan, and R. Philp, 2001, New insights on the Green River petroleum
906 system in the Uinta basin from hydrous pyrolysis experiments: AAPG bulletin, v. 85,
907 no. 8, p. 1333-1371.

908 Selby, D., and R. A. Creaser, 2001, Re-Os geochronology and systematics in molybdenite
909 from the Endako porphyry molybdenum deposit, British Columbia, Canada:
910 Economic Geology, v. 96, no. 1, p. 197-204. DOI: 10.2113/gsecongeo.96.1.197
911 Selby, D., and R. A. Creaser, 2003, Re–Os geochronology of organic rich sediments: an
912 evaluation of organic matter analysis methods: Chemical Geology, v. 200, no. 3-4, p.
913 225-240. DOI: 10.1016/s0009-2541(03)00199-2
914 Selby, D., and R. A. Creaser, 2005a, Direct radiometric dating of hydrocarbon deposits using
915 rhenium-osmium isotopes: Science, v. 308, no. 5726, p. 1293-1295. DOI:
916 10.1126/science.1111081
917 Selby, D., and R. A. Creaser, 2005b, Direct radiometric dating of the Devonian-Mississippian
918 time-scale boundary using the Re-Os black shale geochronometer: Geology, v. 33, no.
919 7, p. 545-548. DOI: 10.1130/g21324.1
920 Selby, D., R. Creaser, K. Dewing, and M. Fowler, 2005, Evaluation of bitumen as a Re–Os
921 geochronometer for hydrocarbon maturation and migration: A test case from the
922 Polaris MVT deposit, Canada: Earth and Planetary Science Letters, v. 235, no. 1-2, p.
923 1-15. DOI: 10.1016/j.epsl.2005.02.018
924 Selby, D., 2007, Direct Rhenium-Osmium age of the Oxfordian-Kimmeridgian boundary,
925 Staffin bay, Isle of Skye, UK, and the Late Jurassic time scale: Norwegian Journal of
926 Geology, v. 87, no. 3, p. 291-299.
927 Selby, D., R. A. Creaser, and M. G. Fowler, 2007, Re–Os elemental and isotopic systematics
928 in crude oils: Geochimica et Cosmochimica Acta, v. 71, no. 2, p. 378-386. DOI:

10.1016/j.gca.2006.09.005

Simpson, G. P., 1999, Sulfate reduction and fluid chemistry of the Devonian Leduc and Nisku formations in south-central Alberta: Ph. D. Dissertation, University of Calgary, Canada, 228 p.

Smoliar, M. I., R. J. Walker, and J. W. Morgan, 1996, Re-Os ages of group IIA, IIIA, IVA, and IVB iron meteorites: Science, v. 271, no. 5252, p. 1099.

Speight, J., 2004, Petroleum Asphaltenes-Part 1: Asphaltenes, resins and the structure of petroleum: Oil & Gas Science and Technology, v. 59, no. 5, p. 467-477. DOI: 10.2516/ogst:2004032

Stasiuk, L. D., 1997, The origin of pyrobitumens in upper Devonian Leduc formation gas reservoirs, Alberta, Canada: An optical and EDS study of oil to gas transformation: Marine and Petroleum Geology, v. 14, no. 7-8, p. 915-929. DOI: 10.1016/S0264-8172(97)00031-7

Stasiuk, L. D., and M. Fowler, 2002, Thermal maturity evaluation (vitrinite and vitrinite reflectance equivalent) of Middle Devonian, Upper Devonian and Devonian-Mississippian strata in the Western Canada Sedimentary basin: Geological Survey of Canada Open File Report 4341, 20 p. DOI: 10.4095/213610

Stoakes, F., and S. Creaney, 1984, Sedimentology of a carbonate source rock: the Duvernay Formation of Central Alberta, *in* L. Eliuk, eds., Carbonates in subsurface and outcrop: Canadian Society of Petroleum Geologists Core Conference, p. 132-147.

Stoakes, F., and S. Creaney, 1985, Controls on the accumulation and subsequent maturation

and migration history of a carbonate source rock. Society of Economic Paleontologists and Mineralogists, *in* Proceedings SEPM Core Workshop Proceedings, Golden, Colorado, p. 343-375.

Switzer, S., W. Holland, D. Christie, G. Graf, A. Hedinger, R. McAuley, R. Wierzbicki, and J. Packard, 1994, Devonian Woodbend-Winterburn strata of the Western Canada sedimentary basin: Geological Atlas of the Western Canada sedimentary basin: Canadian Society of Petroleum Geologists and Alberta Research Council, p. 165-202.

Tozer, R. S., A. P. Choi, J. T. Pietras, and D. J. Tanasichuk, 2014, Athabasca oil sands: Megatrap restoration and charge timing: AAPG Bulletin, v. 98, no. 3, p. 429-447. DOI: 10.1306%2F08071313039

Völkening, J., T. Walczyk, and K.G. Heumann, 1991, Osmium isotope ratio determination by negative thermal ion mass spectrometry: International Journal of Mass Spectrometry and Ion Processes, v. 105, no. 2, p. 147–159. DOI: 10.1016/0168-1176(91)80077-Z

Welte, D. H., B. Horsfield, and D. R. Baker, 2012, Petroleum and basin evolution: insights from petroleum geochemistry, geology and basin modeling: Berlin Heidelberg, Springer, 535 p. DOI: 10.1007/978-3-642-60423-2

Wenger, L. M., C. L. Davis, and G. H. Isaksen, 2001, Multiple controls on petroleum biodegradation and impact on oil quality: Proceedings SPE Annual Technical Conference and Exhibition, 14 p. DOI: 10.2118/71450-MS

Whalen, M. T., G. P. Eberli, F. S. van Buchem, E. W. Mountjoy, and P. W. Homewood, 2000, Bypass margins, basin-restricted wedges, and platform-to-basin correlation, Upper

971 Devonian, Canadian Rocky Mountains: implications for sequence stratigraphy of
972 carbonate platform systems: Journal of Sedimentary Research, v. 70, no. 4, p. 913-
973 936. DOI: 10.1306/2DC40941-0E47-11D7-8643000102C1865D
974 Wu, J., Z. Li, and X. C. Wang, 2016, Comment on “Behavior of Re and Os during contact
975 between an aqueous solution and oil: Consequences for the application of the Re–Os
976 geochronometer to petroleum” by Mahdaoui et al. (2015): Geochimica et
977 Cosmochimica Acta, v. 186, p. 344-347. DOI: 10.1016/j.gca.2016.02.018
978 Ziegler, W., and C. A. Sandberg, 1990, The Late Devonian standard conodont zonation:
979 Courier Forschungsinstitut Senckenberg, v. 121, 115 p.
980

Vitae of authors

Junjie Liu

Department of Earth Sciences, Durham University, Durham, DH1 3LE, UK

junjie.liu@durham.ac.uk

Junjie Liu is currently a postdoctoral research associate at Durham University, UK, focusing on the application and basics of the Re-Os dating of petroleum system. He received his BSc degree and MSc degree from China University of Geosciences, Beijing, and PhD degree from Durham University.

David Selby

Department of Earth Sciences, Durham University, Durham, DH1 3LE, UK

david.selby@durham.ac.uk

Professor David Selby received his BSc in geology from Southampton University, UK and PhD from the University of Alberta, Canada, where is also carried out his postdoctoral research. His research focuses on the application and development of the novel, state-of-the-art, rhenium-osmium radioisotope methodology to the Earth Science disciplines of economic geology, petroleum geoscience and paleoclimate and oceanography.

Mark Obermajer

Geological Survey of Canada, Calgary, Alberta, T2L 2A7, Canada

Mark.Obermajer@NRCan-RNCan.gc.ca

Mark Obermajer is a scientist at the Geological Survey of Canada, Calgary office. He received his MSc degree in geology from Jagiellonian University, Cracow, and a PhD in geology from Western University, Ontario. His scientific interest includes organic geochemistry of hydrocarbon source rocks, oil-oil and oil-source correlations as applied to petroleum systems of Western and Northern Canadian sedimentary basins.

Andy Mort

Geological Survey of Canada, Calgary, Alberta, T2L 2A7, Canada

Andy.Mort@NRCan-RNCan.gc.ca

Dr Andy Mort is a research scientist at the Geological Survey of Canada. He has more than 15 years' experience in conventional and unconventional petroleum systems analysis. His repertoire covers molecular geochemistry applied to oil-oil and oil-source correlation, thermal history modeling and charge evaluation, biodegradation, reservoir formation damage and most recently, the application of geochemistry for fluid phase prediction.

Figure Captions

Figure 1. Map of the study area showing the location of the oil and Duvernay Formation shale samples used in this study (modified from Fowler et al., 2001 with the permission of Canadian Society of Petroleum Geologists). The oils are from the Devonian Leduc and Nisku formations. The majority of the shale samples are located in the mature zone (16-18-52-5W5, 14-29-48-6W5, 2-12-50-26W4 and 2-6-47-4W5) with some from the immature zone (10-27-57-21W4) and the highly mature zone (1-28-36-3W5 and 8-35-31-25W4). Solvent extracts of well 10-27-57-21W4 (low maturity) and 13-14-35-25W4 (high maturity) are used for organic geochemical analysis.

Figure 2. Devonian stratigraphy of the study area, south-central Alberta (information is collectively from the Table of Formations, Alberta by Energy Resources Conservation Board based in Calgary, Canada, Aitken and Norris, 2014, Li et al., 1998 and Fowler et al., 2001). Late Devonian Woodbend Group Duvernay Formation interfingers with Leduc reefs. Also shown here are the organic-rich Devonian-Mississippian Exshaw Formation and the equivalent of Middle Devonian Keg River Formation, the Winnipegosis Formation.

Figure 3. Migration of the Duvernay Formation generated oil (Modified from Switzer et al., 1994 and Rostron, 1997). Following oil generation the Duvernay oil migrated to adjacent Leduc reefs with the underlying Cooking Lake carbonates working as a “pipe line”. In the Bashaw reef area, the differential compaction of the Ireton aquitard due to the underlying Leduc reefs leads to the thinning or absence of the aquitard. This facilitates the breach of Duvernay sourced oil from Leduc reefs to the overlying Nisku formation.

1040 **Figure 4.** Asphaltene content versus asphaltene Re (ppb) and unradiogenic Os (ppt,
1041 represented by ^{192}Os) abundance of the Duvernay oils.

1042 **Figure 5.** $^{187}Re/^{188}Os$ vs $^{187}Os/^{188}Os$ plot for the asphaltene fractions of the Duvernay oil. See
1043 text for discussion.

1044 **Figure 6**. The individually calculated Os_i values of asphaltene samples of the Duvernay oil.
1045 determined at 66 Ma.

1046 **Figure 7**. Duvernay Formation total organic carbon (TOC) (Stasiuk and Fowler, 2002), Re
1047 and unradiogenic Os (^{192}Os as representative) abundances, and calculated $^{187}Os/^{188}Os$
1048 compositions at the time of deposition (Os_i, 378.5 Ma) and oil generation (Os_g, 66 Ma). The
1049 depth of TOC does not correlate exactly with the Re and Os data (Fowler et al., 2003).
1050 Broadly the Re and Os abundances positively co-vary with the TOC content. The Os_i values
1051 show a limited (0.28 to 0.38) range, and yield a weighted average of ~0.33, reflecting a
1052 relatively nonradiogenic $^{187}Os/^{188}Os$ composition for contemporaneous seawater. The Os_g
1053 values of the Duvernay Formation calculated at 66 Ma are between 0.46 and 1.48, and yield a
1054 Tukey's Biweight mean of 0.833 ± 0.009.

1055 **Figure 8a**. Representative gas chromatograms showing distributions of: 1) gasoline range
1056 hydrocarbons and 2) normal alkanes and isoprenoids in low (sample L02221), medium
1057 (sample L02155) and high (sample L02177) maturity Duvernay-sourced crude oils. The high
1058 maturity oils have very low asphaltene content and hence were not selected for Re-Os
1059 analysis. For peak annotations see Table 4.

Figure 8b. Representative gas chromatograms showing distributions of: 3) terpanes and 4) steranes in low (sample L02221), medium (sample L02155) and high (sample L02177) maturity Duvernay-sourced crude oils.

Figure 9. Histogram showing distribution of total organic carbon (TOC) content in the Duvernay Formation samples.

Figure 10. A cross-plot of Rock-Eval hydrogen (HI) and oxygen (OI) indices for the 4 wells from which Re-Os data were collected during present study. The data indicate presence of Type I-II organic matter in most of the samples; notice a systematic decrease in HI values corresponding to an increase in thermal maturity levels from 10-27-57-21W4 and 16-18-52-5W5 through 14-29-48-6W5 to 2-6-47-4W5.

Figure 11. Extract yield data showing relative maturity and source rock potential of the Duvernay Formation samples (criteria by Powell, 1978).

Figure 12. Saturate fraction gas chromatograms showing distributions of 1) normal alkanes and isoprenoids, 2) terpanes and 3) steranes in low and high maturity Duvernay Formation organic extracts. For peak annotations see Table 4.

Figure 13. Oil-source correlation of a Nisku crude oil from Wood River field (within the Bashaw reef complex, 10-28-42-23W4, sample L02203) and Duvernay Formation organic

1081 extract from 13-14-35-25W4 showing strong similarities in the distributions of terpane and
1082 sterane biomarkers. For peak annotations see Table 4.
1083
1084 **Figure 14**. Ternary diagram showing relative normalized abundance of C_{27}:C_{28}:C_{29} regular
1085 steranes based on αββ isomers in the analyzed oil samples. Data for 29 Duvernay extracts
1086 (from GSC-C database) are shown for comparison.

1087 **Figure 15.** $^{187}Re/^{188}Os$ vs $^{187}Os/^{188}Os$ plots for the Duvernay formation. A) core 10-27-57-
1088 21W4; B) core 16-18-52-5W5; C) core 14-29-48-6W5; D) core 2-6-47-4W5; and E) all data
1089 including samples from references (Selby et al., 2007; Finlay et al., 2012). See text for
1090 discussion.

1091 **Figure 16.** Comparison of the currently available $^{187}Os/^{188}Os$ compositions at 66 Ma for the
1092 WCSB Phanerozoic organic-rich intervals shown with the Duvernay shale Os_g and oil Os_i
1093 values.
1094
1095 **Table 1**. Well locations and reservoir formations of the oil samples of this study
1096 **Table 2.** Re-Os data synopsis for the Duvernay Formation shale samples from multiple
1097 locations (wells) and their Os_i (378.5 Ma) and Os_g (66 Ma) values
1098 **Table 3.** Re-Os data synopsis for asphaltene fractions of the oil samples from the Duvernay
1099 petroleum system and their Os_i (66 Ma) values.
1100 **Table 4**. The compounds represented by the peak annotations in the geochemistry figures

1101 (Fig. 8, 12 and 13)

1102 **Table 5.** Re-Os data and calculated $^{187}Os/^{188}Os$ composition at 66 Ma for other oil prone

1103 strata of the WCSB.

Table 1 Well locations and reservoir formations of the oil samples of this study

Sample ID	Well ID	Latitude	Longitude	Depth (m)	Depth (ft)	Formation
L00864	14-35-48-27W4	53.19	-113.85	1920.0-1923.9	6299.2-6312.0	Leduc
L00873	10-9-48-27W4	53.13	-113.89	1781.9-1783.4	5846.1-5851.0	Nisku
L01558	01-3-37-20W4	52.15	-112.77	1604.8-1622.1	5265.1-5321.9	Nisku
L01810	12-11-49-12W5	53.21	-115.66	2997-3069	9833-10069	Nisku
L01827	11-14-42-2W5	52.62	-114.18	2373-2387	7785-7831	Leduc
L01831	8-35-48-12W5	53.18	-115.64	3059-3086	10036-10125	Nisku
L02037	16-16-41-2W5	52.54	-114.22	2431-2442	7976-8012	Nisku
L02083	12-13-41-23W4	52.53	-113.19	1742-1743	5715-5719	Nisku
L02155	10-31-39-23W4	52.4	-113.3	1781.3	5844.2	Nisku
L02196	9-11-33-26W4	51.81	-113.59	2497.8	8194.9	Leduc
L02197	9-14-33-26W4	51.83	-113.58	2202	7224	Nisku
L02203	10-28-42-23W4	52.65	-113.25	1720	5643	Nisku
L02220	11-35-36-20W4	52.14	-112.76	1606.3	5270.0	Nisku
L02221	7-23-36-20W4	52.1	-112.75	1569.7-1617.9	5149.9-5308.1	Leduc/Nisku
L02225	15-22-38-20W4	52.29	-112.78	1563.6-1645.9	5129.9-5399.9	Leduc
L02226	12-10-38-20W4	52.25	-112.79	1569.7-1624.6	5149.9-5330.1	Leduc
L01822	2-27-37-20W4	52.2	-112.78	1599-1603	5246-5259	Leduc

Table 2 Re-Os data synopsis for the Duvernay Formation shale samples from multiple well locations

Sample	Depth (m)	Depth (ft)	Re (ppb)	±	Os (ppt)	±	^{192}Os (ppt)	±	^{187}Re/^{188}Os	±	^{187}Os/^{188}Os	±	rho [a]	Os_i [b]	±	Os_g [c]	±
10-27-57-21W4			*53.96°N*		*113.03°W*												
DS18-12	1106	3629	5.84	0.02	631.2	2.2	244.5	1.0	47.5	0.2	0.633	0.004	0.590	0.33	0.01	0.58	0.01
DS20-12	1125	3691	14.37	0.04	1245.3	4.8	478.7	2.2	59.7	0.3	0.693	0.005	0.604	0.32	0.01	0.63	0.01
DS22-12	1128	3701	13.23	0.04	1299.2	5.1	500.7	2.4	52.5	0.3	0.673	0.005	0.600	0.34	0.01	0.62	0.01
DS24-12	1140	3740	12.36	0.04	1121.1	4.4	431.3	2.1	57.0	0.3	0.687	0.005	0.600	0.33	0.01	0.62	0.01
DS26-12	1144	3753	16.86	0.05	947.8	3.8	355.5	1.5	94.4	0.5	0.899	0.005	0.598	0.30	0.01	0.80	0.01
DS28-12	1146	3760	14.68	0.04	1392.9	5.2	537.7	2.4	54.3	0.3	0.659	0.004	0.598	0.32	0.01	0.60	0.01
DS30-12	1151	3776	26.33	0.07	1965.2	6.9	751.1	2.9	69.8	0.3	0.742	0.004	0.584	0.30	0.01	0.67	0.01
DS32-12	1154	3786	24.15	0.06	1537.6	5.6	579.5	2.2	82.9	0.4	0.859	0.005	0.582	0.34	0.01	0.77	0.01
DS34-12	1160	3806	10.91	0.03	397.1	2.0	142.7	0.7	152.0	0.9	1.267	0.009	0.608	0.31	0.02	1.10	0.01
DS36-12	1161	3809	25.43	0.07	1188.0	4.7	436.5	1.7	115.9	0.5	1.074	0.006	0.582	0.34	0.01	0.95	0.01
16-18-52-5W5			*53.5°N*		*114.72°W*												
DS1-12	2343.0	7687.0	0.31	0.01	58.8	2.1	23.2	1.9	26.3	2.2	0.488	0.055	0.687	0.32	0.07	0.46	0.06
DS3-12	2343.5	7689.6	1.25	0.01	242.5	2.5	95.6	1.9	26.0	0.5	0.491	0.014	0.683	0.33	0.02	0.46	0.02
DS5-12	2344.0	7690.3	2.03	0.01	178.1	1.3	68.5	0.8	58.9	0.7	0.693	0.012	0.671	0.32	0.02	0.63	0.01
DS7-12	2344.5	7691.9	4.03	0.01	248.0	1.3	93.4	0.7	85.8	0.7	0.862	0.009	0.657	0.32	0.01	0.77	0.01
14-29-48-6W5			*53.18°N*		*114.85°W*												
DS9-12	2646.6	8683.1	48.46	0.14	1370.7	8.2	474.1	2.9	203.3	1.4	1.611	0.014	0.646	0.32	0.02	1.39	0.02
DS11-12	2648.6	8689.6	8.75	0.03	362.4	1.9	132.7	0.8	131.3	0.9	1.107	0.010	0.622	0.28	0.02	0.96	0.01
DS13-12	2650.6	8696.2	10.82	0.03	482.0	2.3	176.0	0.9	122.3	0.7	1.129	0.008	0.609	0.36	0.01	0.99	0.01
DS15-12	2652.6	8702.8	21.94	0.06	1827.3	6.6	700.6	2.8	62.3	0.3	0.716	0.004	0.576	0.32	0.01	0.65	0.01
DS17-12	2654.6	8709.3	36.35	0.09	1726.5	8.7	636.2	3.4	113.7	0.7	1.050	0.009	0.589	0.33	0.01	0.93	0.01

2-6-47-4W5			*53.02°N*		*114.57°W*												
DS37-12	2629	8625	0.53	0.01	29.0	1.0	10.8	0.9	98.2	8.0	0.942	0.107	0.701	0.32	0.16	0.83	0.12
DS38-12	2631	8632	0.40	0.01	30.7	0.7	11.7	0.6	68.2	3.6	0.792	0.056	0.677	0.36	0.08	0.72	0.06
DS39-12	2633	8638	1.36	0.01	62.2	0.9	22.8	0.6	118.5	3.2	1.110	0.042	0.694	0.36	0.06	0.98	0.05
DS40-12	2635	8645	41.52	0.14	1218.3	4.2	423.1	1.0	195.2	0.8	1.575	0.005	0.403	0.34	0.01	1.36	0.01
DS41-12	2637	8652	67.56	0.22	1721.5	7.0	587.5	1.7	228.8	1.0	1.736	0.007	0.476	0.29	0.01	1.48	0.01
DS42-12	2639	8658	13.07	0.04	900.4	2.9	340.3	1.1	76.4	0.3	0.836	0.004	0.486	0.35	0.01	0.75	0.01
DS43-12	2641	8665	11.27	0.04	746.9	3.7	282.3	1.8	79.4	0.6	0.835	0.007	0.620	0.33	0.01	0.75	0.01
DS44-12	2643	8671	5.99	0.02	430.7	1.8	163.0	0.8	73.1	0.4	0.823	0.006	0.576	0.36	0.01	0.74	0.01
DS45-12	2645	8678	8.74	0.03	598.6	3.5	226.1	1.8	76.9	0.7	0.841	0.010	0.648	0.35	0.01	0.76	0.01
DS46-12	2647	8684	28.75	0.09	1707.7	5.7	639.0	2.0	89.5	0.4	0.919	0.004	0.482	0.35	0.01	0.82	0.01
DS47-12	2649	8691	41.79	0.14	1774.0	8.1	649.0	3.1	128.1	0.7	1.112	0.008	0.581	0.30	0.01	0.97	0.01
2-12-50-26W4 [d]			*53.30°N*		*113.67°W*												
DS44-03	1751.6	5746.7	7.41	0.03	383	2	140	1	104.4	0.6	1.037	0.006	0.800	0.38	0.01	0.92	0.01
8-35-31-25W4 [d]			*51.70°N*		*113.43°W*												
DS69-03	2340.9	7680.1	11.55	0.04	569	2	208	1	109.5	0.5	1.036	0.004	0.800	0.34	0.01	0.92	0.01
1-28-36-3W5 [e]			*52.20°N*		*114.60°W*												
DS45-03-1-4	3013.1	9885.5	8.10	0.03	219.6	1.2	75.3	0.4	214.1	1.2	1.689	0.012	0.542	0.34	0.02	1.45	0.01

[a] rho: error correlation value between $^{187}Re/^{188}Os$ and $^{187}Os/^{188}Os$;

[b] Os_i = initial $^{187}Os/^{188}Os$ ratio of shales during deposition which is calculated at 378.5 Ma (see text for discussion);

[c] Os_g = $^{187}Os/^{188}Os$ ratio of shales at oil generation calculated at 66 Ma (see text for discussion);

[d] Data from Finlay et al. (2012);

[e] Data from Selby et al. (2007).

Table 3 Re-Os data synopsis for asphaltene fractions of the oil samples from the Duvernay petroleum system

Sample ID	Asphaltene (%)	Re (ppb)	±	Os (ppt)	±	^{192}Os (ppt)	±	^{187}Re/^{188}Os	±	^{187}Os/^{188}Os	±	rho [a]	Os_i [b]	±
L00864	1.61%	0.12	0.07	9.4	0.5	3.6	0.5	66.8	37.1	0.775	0.111	0.211	0.70	0.15
L00864rpt	1.16%	0.13	0.05	8.2	0.4	3.0	0.3	84.9	31.1	0.980	0.118	0.270	0.89	0.15
L00864rpt2	1.81%	0.12	0.04	7.4	0.4	2.7	0.4	84.1	32.0	1.036	0.164	0.291	0.94	0.20
L00873	5.65%	0.42	0.03	8.8	0.3	3.3	0.2	256.1	26.1	1.006	0.086	0.621	0.72	0.12
L01558	3.60%	1.42	0.03	20.4	0.5	7.6	0.4	371.1	20.0	0.970	0.063	0.698	0.56	0.09
L02083	2.46%	1.26	0.04	11.2	0.4	3.9	0.3	641.6	51.8	1.521	0.131	0.814	0.82	0.19
L02155	1.45%	0.32	0.04	3.6	0.3	1.2	0.3	511.4	131.1	1.623	0.373	0.844	1.06	0.52
L02196	0.25%	0.04	0.00	0.6	0.1	0.2	0.1	351.4	81.0	1.105	0.275	0.918	0.72	0.36
L02203	1.39%	0.26	0.00	4.6	0.5	1.7	0.5	298.8	85.4	0.878	0.273	0.919	0.55	0.37
L02220	3.00%	1.41	0.03	19.1	0.5	7.0	0.4	400.4	22.9	1.105	0.073	0.712	0.66	0.10
L02221 [c]	14.10%	3.78	0.04	41.2	1.6	14.9	1.2	504.7	42.3	1.206	0.139	0.712	0.65	0.19
L02225 [c]	6.75%	0.51	0.04	6.4	0.4	2.3	0.3	442.6	74.5	1.285	0.219	0.760	0.80	0.30
L02226 [c]	5.84%	1.11	0.05	12.0	0.6	4.2	0.5	524.6	68.6	1.475	0.216	0.766	0.90	0.29
L01822 [d]	14.50%	2.03	0.07	25.3	1.6	8.8	0.6	457.1	72.3	1.488	0.236	0.500	0.99	0.32
Data not applied on isochron														
L01810	0.35%	0.04	0.11	1.0	0.8			218.2	705.6	0.63	1.33	0.54		
L01831	0.52%	0.01	0.11	23.3	1.0			2.0	25.1	1.11	0.12	0.01		
L02196rpt	0.78%	0.02	0.05	0.6	0.4			210.4	562.6	0.52	0.92	0.51		
L02037	0.28%	0.05	0.17	-	-			-	-	-	-	-		
L02197	0.27%	0.07	0.17	-	-			-	-	-	-	-		

[a] rho: error correlation value between ^{187}Re/^{188}Os and ^{187}Os/^{188}Os;

[b] Osi = initial ^{187}Os/^{188}Os ratios of oil at the timing of generation which are calculated at 66 Ma (see text for discussion);

[c] these samples are asphaltene fractions precipitated by *n*-pentane at the GSC;

[d] data from Selby et al. (2007).

Table 4 The compounds represented by the peak annotations in the geochemistry figures (Fig. 8-10)

Peak	**Compound**	**Peak**	**Compound**
n-C_5	C_5 *n*-alkane	C_{26}TT	C_{26} tricyclic terpane
n-C_6	C_6 *n*-alkane	Ts	18α(H),22,29,30-trisnorhopane (Ts)
MCYC5	methylcyclopentane	Tm	17α(H),22,29,30-trisnorhopane (Tm)
n-C_7	C_7 *n*-alkane	C_{29}	17α(H),21β(H)-30-norhopane
MCYC6	methylcyclohexane	C_{29}Ts	18α(H),21β(H)-norneohopane
n-C_8	C_8 *n*-alkane	C_{30}H	17α(H),21β(H)-hopane
Pr	pristane	G	gammacerane
Ph	phytane	C_{34}	17α(H),21β(H)-tetrakishomohopanes
n-C_{15}	C_{15} *n*-alkane	C_{35}	17α(H),21β(H)-pentakishomohopanes
n-C_{20}	C_{20} *n*-alkane	C_{21}P	pregnane
n-C_{25}	C_{25} *n*-alkane	dC_{27}S20S	diacholestane 20S
C_{23}TT	C_{23} tricyclic terpane	dC_{29}S20S	diastigmastane 20S
C_{24}TeT	C_{24} tetracyclic terpane	C_{29}S20R	5α(H),14β(H),17β(H)-stigmastane 20R

Table 5 Re-Os data and calculated $^{187}Os/^{188}Os$ composition at 66 Ma (Os_g) for other oil prone strata of the WCSB

Lower Jurassic Gordondale Member

Finlay et al. (2012)

wells	depth (m)	depth (ft)	Re (ppb)	Os (ppt)	$^{187}Re/^{188}Os$	$^{187}Os/^{188}Os$	Os_g [a]
07-31-79-10W6	1557.0	5108.3	574.9	6.34	550.4	2.116	1.51
14-24-80-7W6	1183.5	3882.9	369.2	1.86	1674	5.900	4.06
14-24-80-7W6	1190.4	3905.5	229.9	1.83	885.8	3.655	2.68
8-26-69-7W6	2271.4	7452.1	195.3	6.13	178.6	1.372	1.18
10-17-84-22W5	2361.0	7746.1	196.2	1.12	1352	4.748	3.26
6-29-85-11W5	1148.7	3768.7	402.6	3.05	933.2	3.716	2.69

Selby et al. (2007) [b] *well 6-32-78-5W6 1218.0-1218.6 m (3996.1-3998.0 ft)*

sample	$^{187}Re/^{188}Os$	$^{187}Os/^{188}Os$	Os_g [a]
TS22b.DD.GB	765.25	2.925	2.08
TS23c.DD.GB	432.40	1.914	1.44
TS24b.DD.GB	291.71	1.405	1.08
TS25b.DD.GB	424.18	1.926	1.46
TS26a.DD.GB	182.21	1.186	0.99

Devonian-Mississippian Exshaw Formation

Selby and Creaser (2005) 51°05'29''N 115°09'29''W

within ~4 m (13 ft) lateral interval and 10 cm (0.4 in) of vertical stratigraphy

sample	Re (ppb)	Os (ppt)	$^{187}Re/^{188}Os$	$^{187}Os/^{188}Os$	Os_g [a]
DS53	15.6	367.8	253.5	1.948	1.67
DS54	17.5	375.9	283.8	2.141	1.83
DS55A	15.5	341.4	273.7	2.073	1.77
DS55B	16.4	363.5	277.3	2.100	1.80
DS55C	21.2	426.3	306.1	2.265	1.93
DS56	16.4	493.3	190.4	1.570	1.36
DS57	36.0	595.8	391.8	2.787	2.36
DS58A	15.2	458.7	189.3	1.563	1.35
DS58B	16.6	490.6	194.5	1.597	1.38

Selby et al. (2003); Creaser et al. (2002); Finlay et al. (2012)

wells	depth (m)	depth (ft)	Re (ppb)	Os (ppb)	$^{187}Re/^{188}Os$	$^{187}Os/^{188}Os$	Os_g [a]
3-19-80-23W5	1752.0	5748.0	70.0	0.69	487.1	3.517	2.98
3-19-80-23W5	1753.0	5751.3	88.8	1.62	350.7	2.656	2.27
3-19-80-23W5	1754.0	5754.6	22.8	0.50	279.8	2.195	1.89
3-19-80-23W5	1756.5	5762.8	31.7	0.48	441.1	3.220	2.73
13-18-80-23W5	1748.8	5737.5	47.9	0.64	518.3	3.546	2.98
13-18-80-23W5	1750.9	5744.4	68.9	1.11	408.9	2.987	2.54
8-29-78-01W6	2099.1	6886.8	128.6	1.70	538.4	3.806	3.21

8-29-78-01W6	2099.2	6887.1	20.0	0.69	166.1	1.535	1.35
14-22-80-02W6	2058.3	6753.0	31.8	0.67	287.5	2.095	1.78
6-19-78-25W5	2006.2	6582.0	52.0	0.84	405.1	2.885	2.44
4-23-72-10W6	3570.4	11713.9	31.3	0.29	916.8	5.968	4.96
4-23-72-10W6	3567.7	11705.1	42.3	0.80	327.8	2.389	2.03

Middle Devonian Keg River Formation, La Crete Basin

Miller (2004)

sample ID	Re (ppb)	Os (ppb)	$^{187}Re/^{188}Os$	$^{187}Os/^{188}Os$	Os_g [a]
CM-KR-1	50.8	1.24	238	1.775	1.51
CM-KR-2	34.6	0.94	208	1.568	1.34
CM-KR-3	32.8	0.92	204	1.575	1.35
CM-KR-4	20.7	0.47	259	1.920	1.64
CM-KR-5	57.2	0.95	386	2.733	2.31
CM-KR-6	224.2	2.32	757	5.087	4.25
CM-KR-7	26.7	0.67	232	1.754	1.50
CM-KR-I-D	42.4	0.78	336	2.392	2.02
CM-KR-I-E	37.9	0.78	294	2.124	1.80

Ordovician Kukersites, Williston Basin

Miller (2004)

sample ID	Re (ppb)	Os (ppb)	$^{187}Re/^{188}Os$	$^{187}Os/^{188}Os$	Os_g [a]
CM-13	2.60	0.085	146	1.608	1.45
CM-14	0.94	0.033	136	1.390	1.24
CM-15	1.01	0.031	155	1.742	1.57
CM-16 (rpt.)	0.60	0.069	44.7	0.776	0.73
CM-17 (rpt.)	0.27	0.074	18.5	0.476	0.46
CM-19 (rpt.)	0.40	0.063	31.4	0.514	0.48
CM-22 (rpt.)	0.40	0.067	30.2	0.580	0.55
CM-IV-A-iii.iv.v (rpt.)	0.22	0.019	54.7	0.899	0.84
CM-IV-A-v,vi,vii (rpt.)	0.24	0.023	50	0.894	0.84
CM-IV-A-xiii,xiv,xv	0.23	0.015	75.6	0.943	0.86
CM-IV-A-xvi	0.14	0.030	22.4	0.593	0.57
CM-24	6.58	0.070	752	6.190	5.36
CM-28	0.50	0.048	49.5	0.845	0.79

Neoproterozoic Old Fort Point Formation, Jasper, Alberta

Kendall et al. (2004) *52.96°N* *118.48°W*

samples	Re (ppb)	Os (ppt)	$^{187}Re/^{188}Os$	$^{187}Os/^{188}Os$	Os_g [a]	Os_i [c]
BK-01-014B	15.43	249.4	524.7	5.954	5.38	0.61
BK-01-015A	6.36	164.7	262.9	3.299	3.01	0.62
BK-01-015B	12.53	218.9	463.7	5.352	4.84	0.63
BK-01-015C	8.54	192.0	318.7	3.859	3.51	0.61
BK-01-015D	7.28	144.8	379.6	4.475	4.06	0.61

[a] Os_g = $^{187}Os/^{188}Os$ ratios of strata at the approximate timing of thermal maturation of most of the strata (adopting the Re-Os age of 66 Ma);
[b] No Re and Os abundance data available;
[c] Os_i = initial $^{187}Os/^{188}Os$ ratios of Old Fort Point Formation calculated at its Re-Os depositional age of 608 Ma.

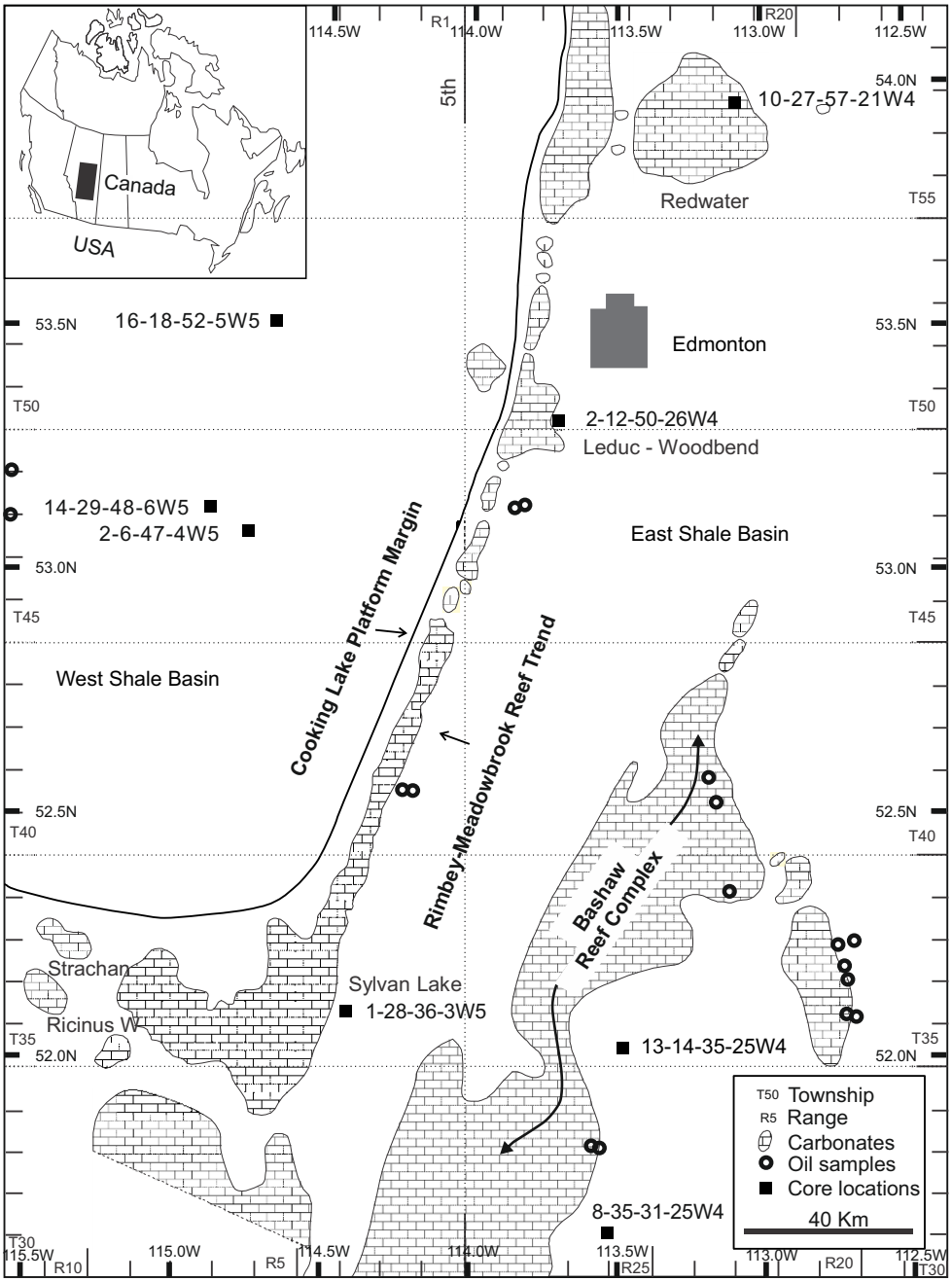
Canada
USA
114.5W
R1
114.0W
5th
113.5W
R20
113.0W
112.5W
54.0N
10-27-57-21W4
Redwater
T55
53.5N
16-18-52-5W5
Edmonton
53.5N
T50
T50
2-12-50-26W4
Leduc - Woodbend
14-29-48-6W5
2-6-47-4W5
East Shale Basin
53.0N
53.0N
T45
T45
West Shale Basin
Cooking Lake Platform Margin
Rimbey-Meadowbrook Reef Trend
Bashaw Reef Complex
52.5N
52.5N
T40
T40
Strachan
Ricinus W
Sylvan Lake
1-28-36-3W5
13-14-35-25W4
T35
52.0N
T35
52.0N
T50 Township
R5 Range
Carbonates
Oil samples
Core locations
40 Km
8-35-31-25W4
T30
115.5W
R10
115.0W
R5
114.5W
114.0W
113.5W
R25
113.0W
R20
112.5W
T30

Figure 1

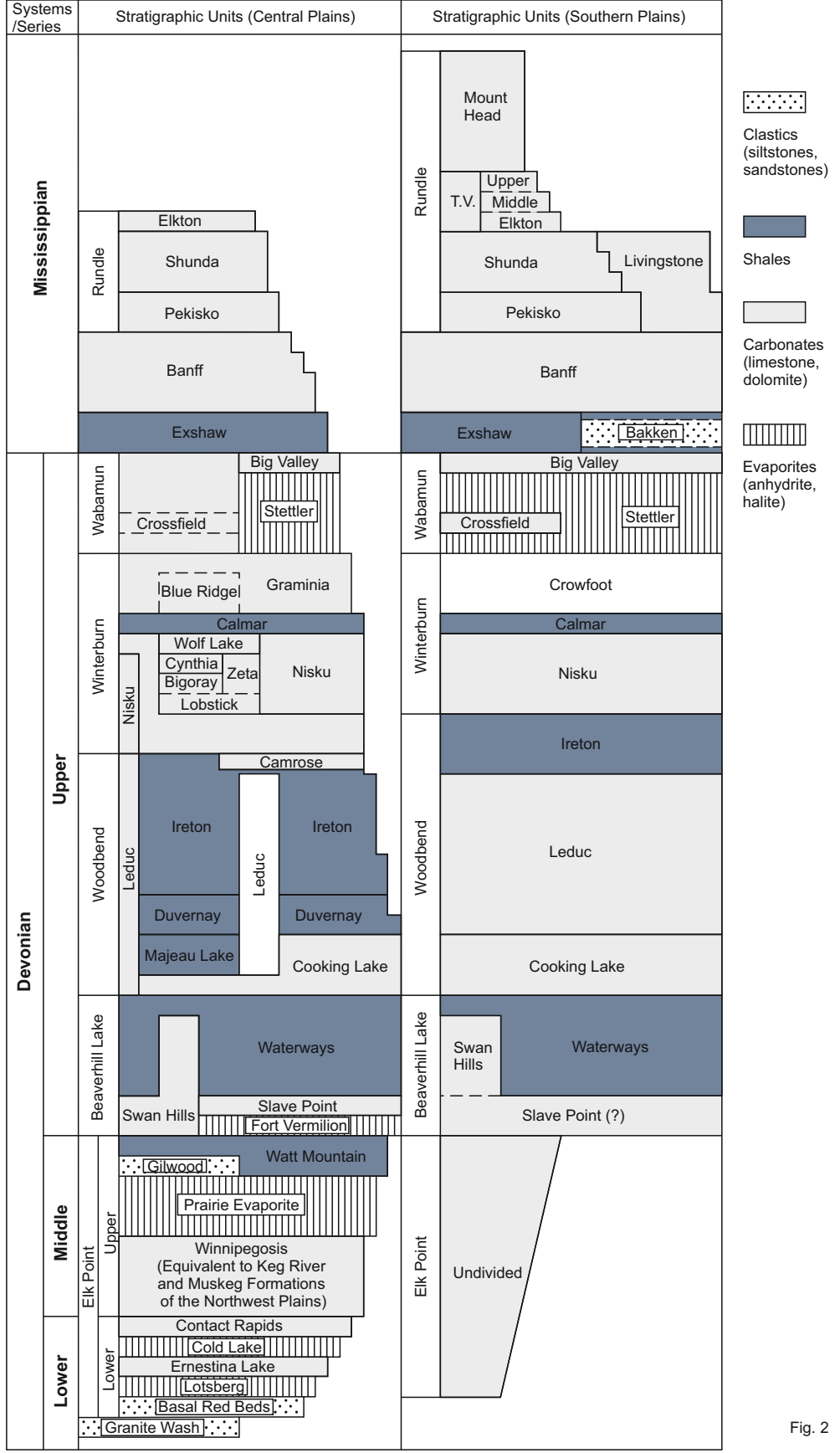
Systems /Series
Stratigraphic Units (Central Plains)
Stratigraphic Units (Southern Plains)
Mississippian
Devonian
Upper
Middle
Lower
Rundle
Elkton
Shunda
Pekisko
Banff
Exshaw
Mount Head
T.V.
Upper
Middle
Elkton
Livingstone
Bakken
Wabamun
Big Valley
Crossfield
Stettler
Winterburn
Blue Ridge
Graminia
Crowfoot
Calmar
Wolf Lake
Cynthia
Bigoray
Zeta
Lobstick
Nisku
Woodbend
Camrose
Ireton
Leduc
Duvernay
Majeau Lake
Cooking Lake
Beaverhill Lake
Waterways
Swan Hills
Slave Point
Slave Point (?)
Fort Vermilion
Elk Point
Gilwood
Watt Mountain
Prairie Evaporite
Winnipegosis
(Equivalent to Keg River
and Muskeg Formations
of the Northwest Plains)
Undivided
Contact Rapids
Cold Lake
Ernestina Lake
Lotsberg
Basal Red Beds
Granite Wash
Clastics
(siltstones,
sandstones)
Shales
Carbonates
(limestone,
dolomite)
Evaporites
(anhydrite,
halite)

Fig. 2

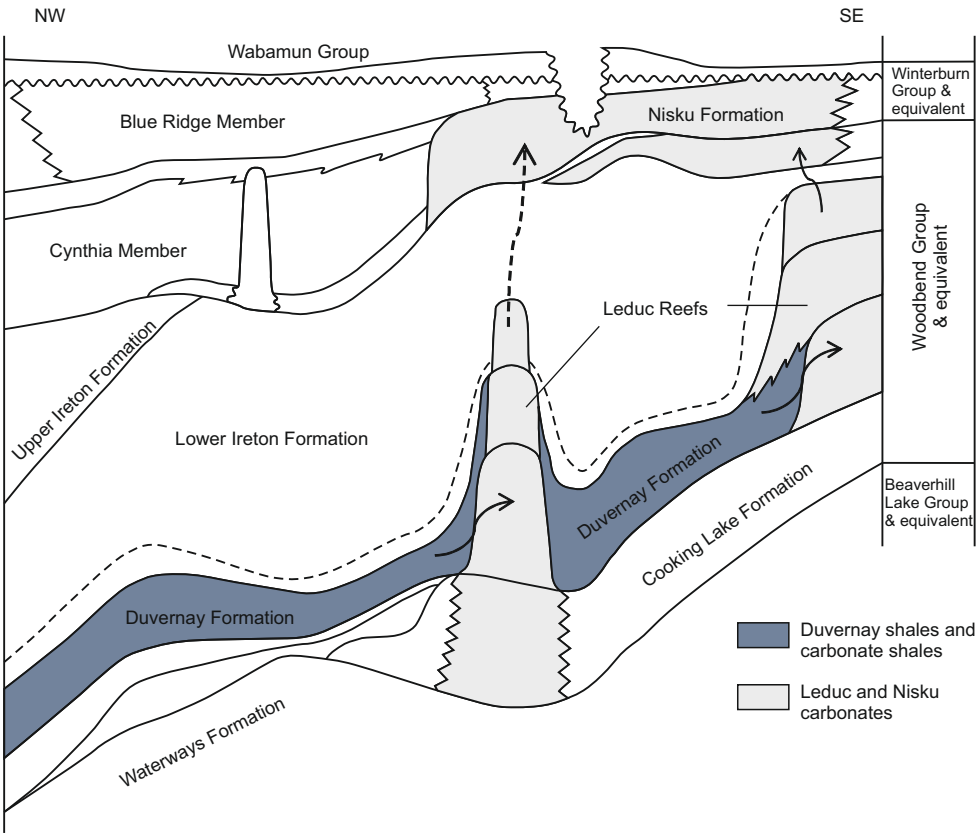
NW
SE
Wabamun Group
Blue Ridge Member
Nisku Formation
Winterburn Group & equivalent
Cynthia Member
Leduc Reefs
Woodbend Group & equivalent
Upper Ireton Formation
Lower Ireton Formation
Duvernay Formation
Cooking Lake Formation
Beaverhill Lake Group & equivalent
Duvernay Formation
Waterways Formation
Duvernay shales and carbonate shales
Leduc and Nisku carbonates

Figure 3

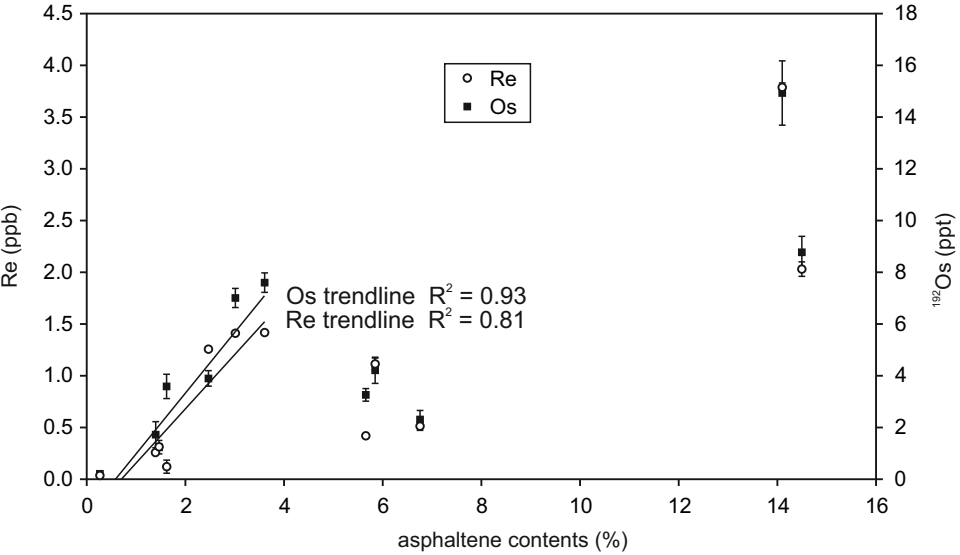
Re (ppb)
^{192}Os (ppt)
asphaltene contents (%)
Re
Os
Os trendline R^2 = 0.93
Re trendline R^2 = 0.81
0.0
0.5
1.0
1.5
2.0
2.5
3.0
3.5
4.0
4.5
0
2
4
6
8
10
12
14
16
18

Figure 4

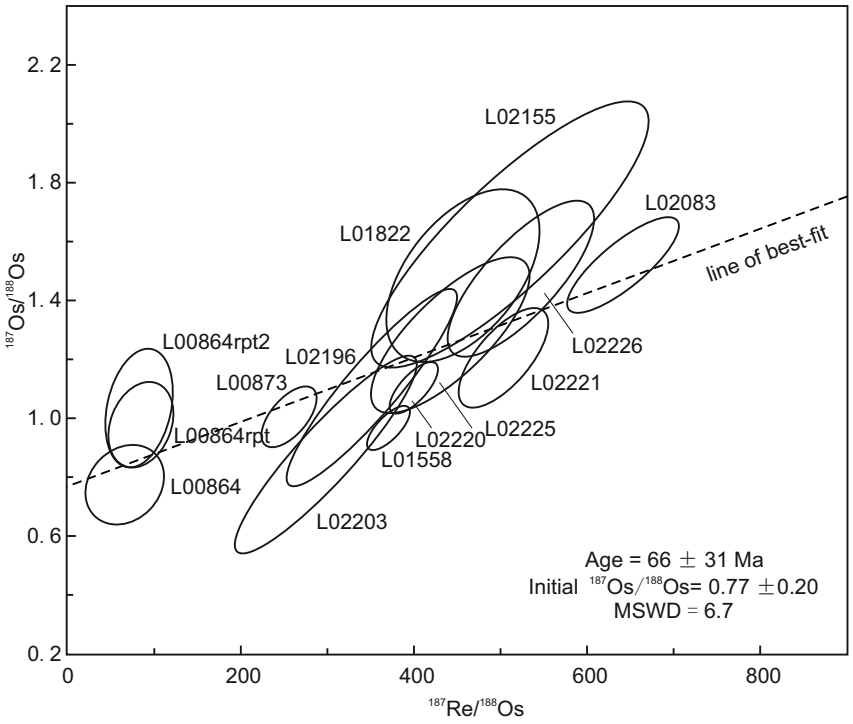
2. 2
1. 8
1. 4
1. 0
0. 6
0. 2
0
200
400
600
800
$^{187}Os/^{188}Os$
$^{187}Re/^{188}Os$
L02155
L02083
L01822
line of best-fit
L00864rpt2
L02196
L02226
L00873
L02221
L00864rpt
L02220
L02225
L01558
L00864
L02203
Age = 66 ± 31 Ma
Initial $^{187}Os/^{188}Os$= 0.77 ±0.20
MSWD = 6.7

Figure 5

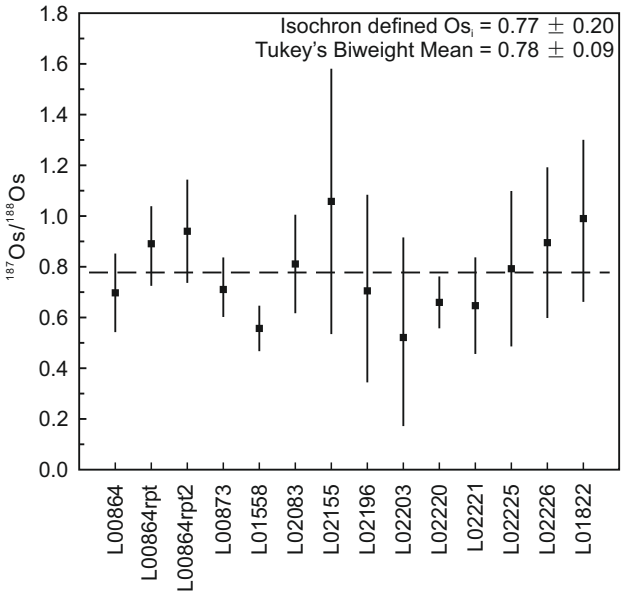
Isochron defined Os$_i$ = 0.77 ± 0.20
Tukey's Biweight Mean = 0.78 ± 0.09
$^{187}Os/^{188}Os$
1.8
1.6
1.4
1.2
1.0
0.8
0.6
0.4
0.2
0.0
L00864
L00864rpt
L00864rpt2
L00873
L01558
L02083
L02155
L02196
L02203
L02220
L02221
L02225
L02226
L01822

Figure 6

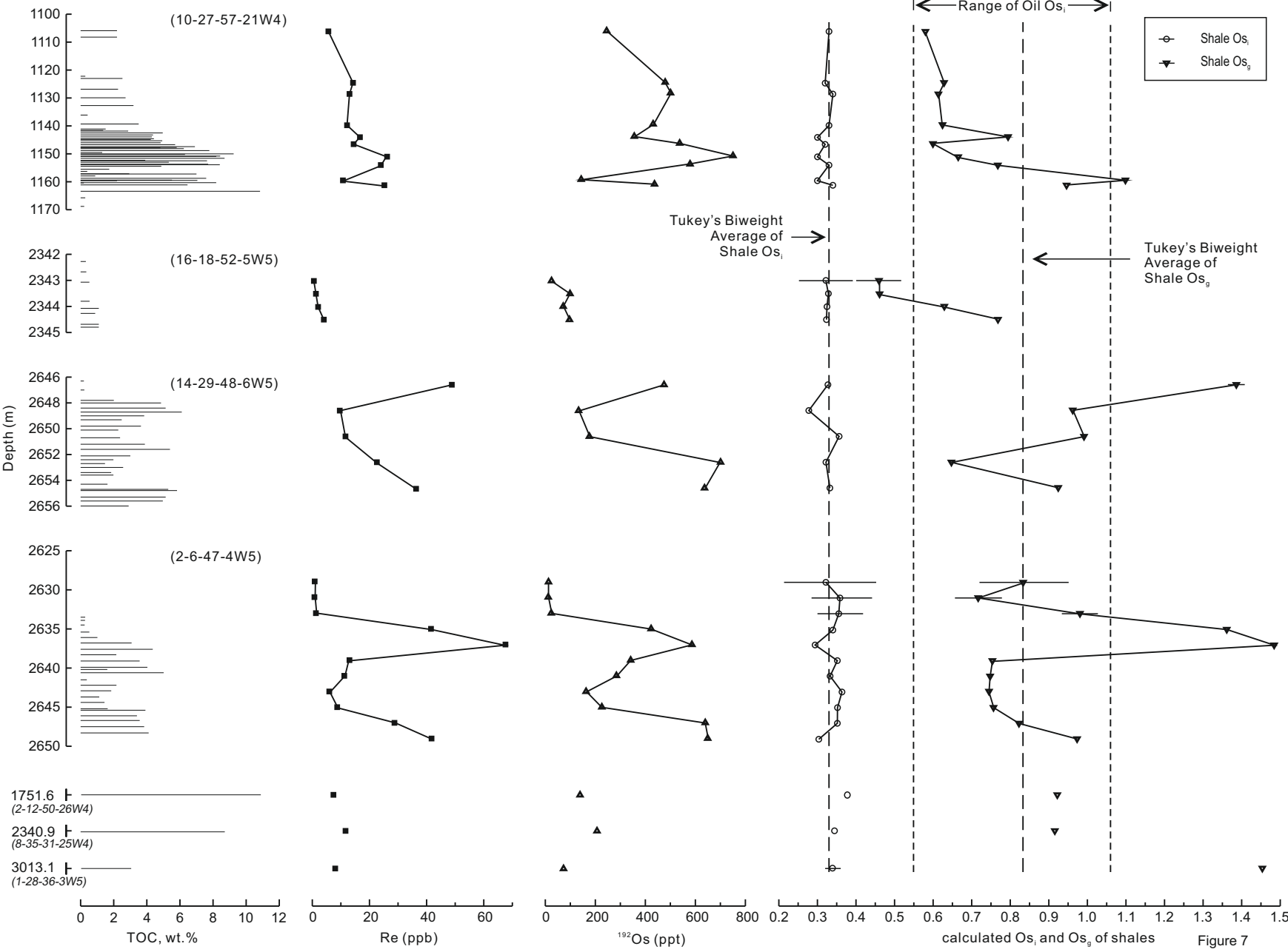
(10-27-57-21W4)
(16-18-52-5W5)
(14-29-48-6W5)
(2-6-47-4W5)
Depth (m)
1100
1110
1120
1130
1140
1150
1160
1170
2342
2343
2344
2345
2646
2648
2650
2652
2654
2656
2625
2630
2635
2640
2645
2650
1751.6
(2-12-50-26W4)
2340.9
(8-35-31-25W4)
3013.1
(1-28-36-3W5)
Range of Oil Os$_i$
Shale Os$_i$
Shale Os$_g$
Tukey's Biweight Average of Shale Os$_i$
Tukey's Biweight Average of Shale Os$_g$
0 2 4 6 8 10 12
TOC, wt.%
0 20 40 60
Re (ppb)
0 200 400 600 800
^{192}Os (ppt)
0.2 0.3 0.4 0.5 0.6 0.7 0.8 0.9 1.0 1.1 1.2 1.3 1.4 1.5
calculated Os$_i$ and Os$_g$ of shales

Figure 7

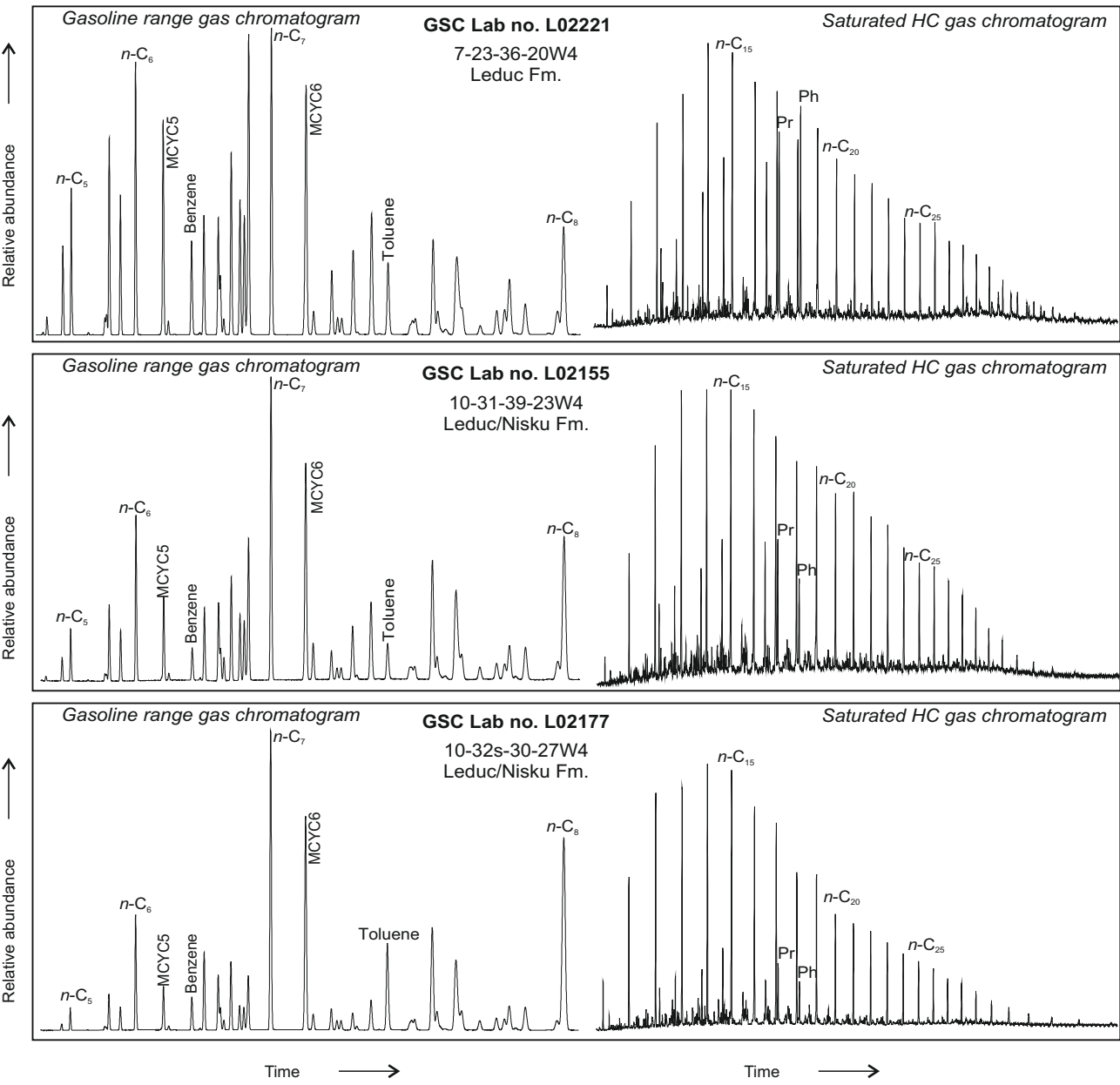
Gasoline range gas chromatogram
GSC Lab no. L02221
7-23-36-20W4
Leduc Fm.
Saturated HC gas chromatogram
Relative abundance
n-C5
n-C6
MCYC5
Benzene
n-C7
MCYC6
Toluene
n-C8
n-C15
Pr
Ph
n-C20
n-C25
Gasoline range gas chromatogram
GSC Lab no. L02155
10-31-39-23W4
Leduc/Nisku Fm.
Saturated HC gas chromatogram
Relative abundance
n-C5
n-C6
MCYC5
Benzene
n-C7
MCYC6
Toluene
n-C8
n-C15
Pr
Ph
n-C20
n-C25
Gasoline range gas chromatogram
GSC Lab no. L02177
10-32s-30-27W4
Leduc/Nisku Fm.
Saturated HC gas chromatogram
Relative abundance
n-C5
n-C6
MCYC5
Benzene
n-C7
MCYC6
Toluene
n-C8
n-C15
Pr
Ph
n-C20
n-C25
Time
Time

Figure 8a

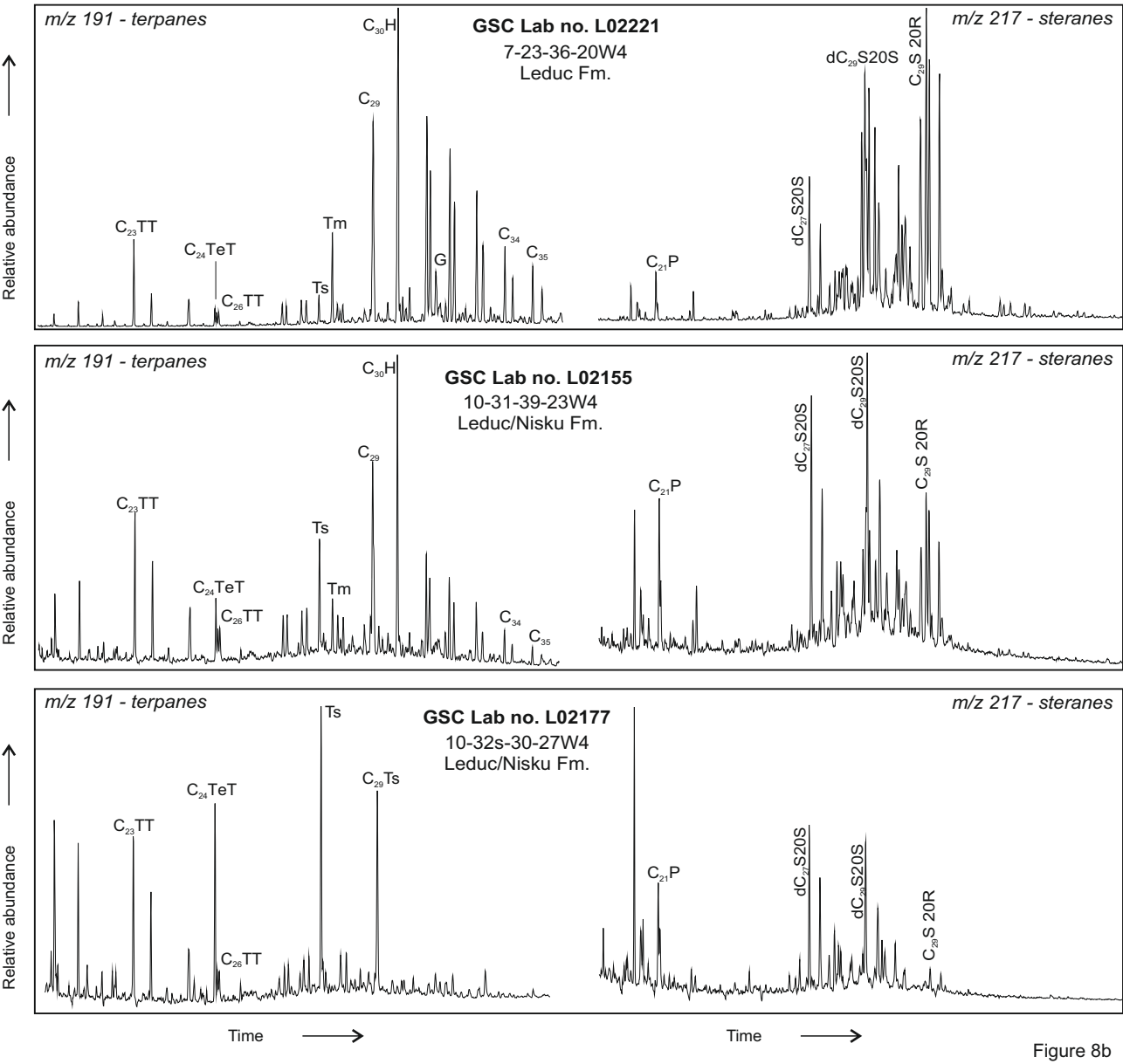
m/z 191 - terpanes
GSC Lab no. L02221
7-23-36-20W4
Leduc Fm.
m/z 217 - steranes
Relative abundance
C23TT
C24TeT
C26TT
Ts
Tm
C30H
C29
G
C34
C35
C21P
dC27S20S
dC29S20S
C29 S 20R
m/z 191 - terpanes
GSC Lab no. L02155
10-31-39-23W4
Leduc/Nisku Fm.
m/z 217 - steranes
Relative abundance
C23TT
C24TeT
C26TT
Ts
Tm
C30H
C29
C34
C35
C21P
dC27S20S
dC29S20S
C29 S 20R
m/z 191 - terpanes
GSC Lab no. L02177
10-32s-30-27W4
Leduc/Nisku Fm.
m/z 217 - steranes
Relative abundance
C23TT
C24TeT
C26TT
Ts
C29Ts
C21P
dC27S20S
dC29S20S
C29 S 20R
Time
Time

Figure 8b

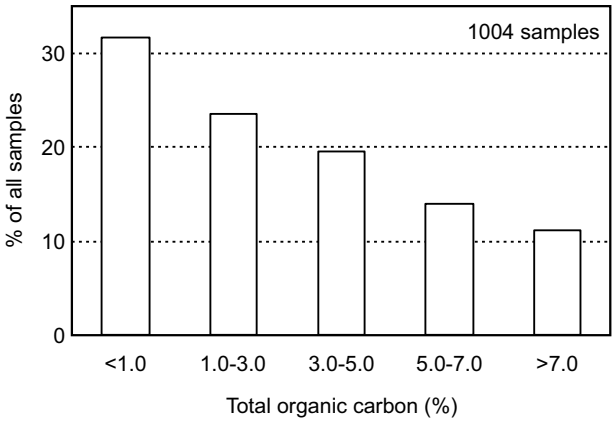
1004 samples
30
20
10
0
% of all samples
<1.0
1.0-3.0
3.0-5.0
5.0-7.0
>7.0
Total organic carbon (%)

Figure 9

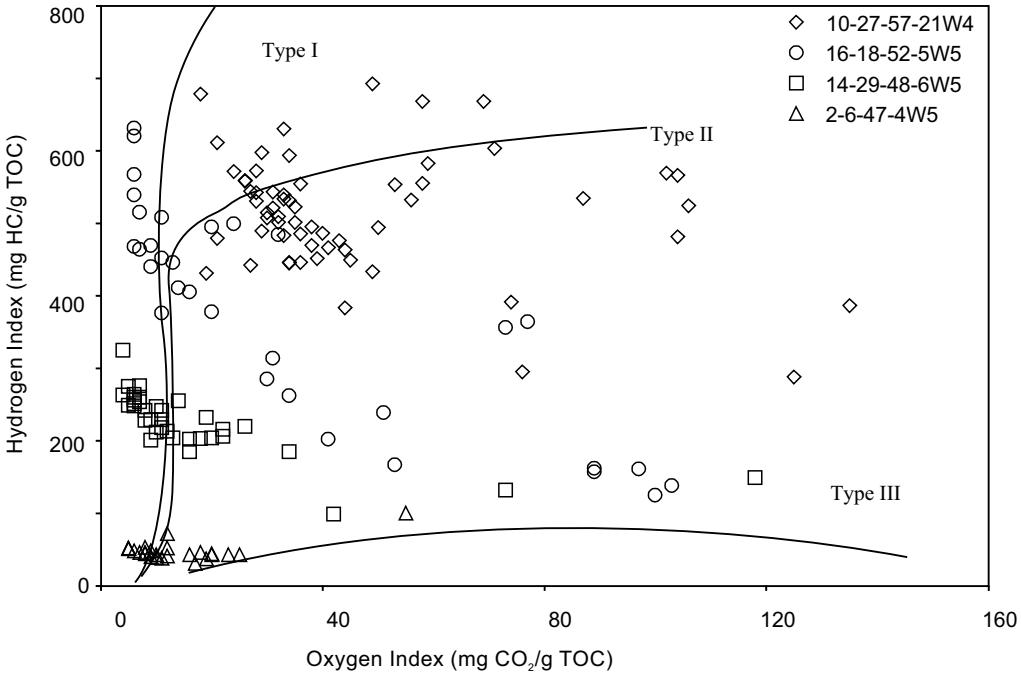
Type I
Type II
Type III
10-27-57-21W4
16-18-52-5W5
14-29-48-6W5
2-6-47-4W5
Hydrogen Index (mg HC/g TOC)
Oxygen Index (mg CO2/g TOC)
800
600
400
200
0
0
40
80
120
160

Figure 10

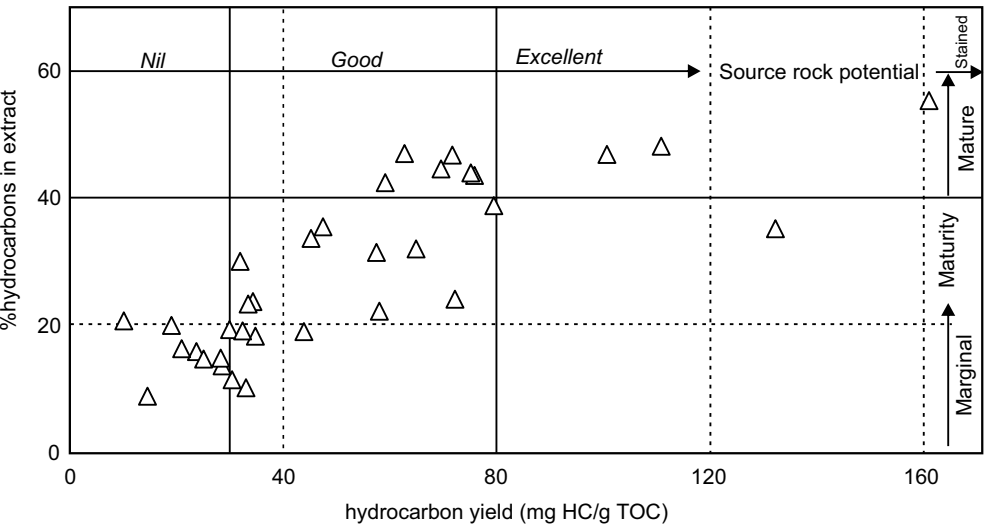
Nil
Good
Excellent
Source rock potential
Stained
Mature
Maturity
Marginal
%hydrocarbons in extract
hydrocarbon yield (mg HC/g TOC)
0
20
40
60
0
40
80
120
160

Figure 11

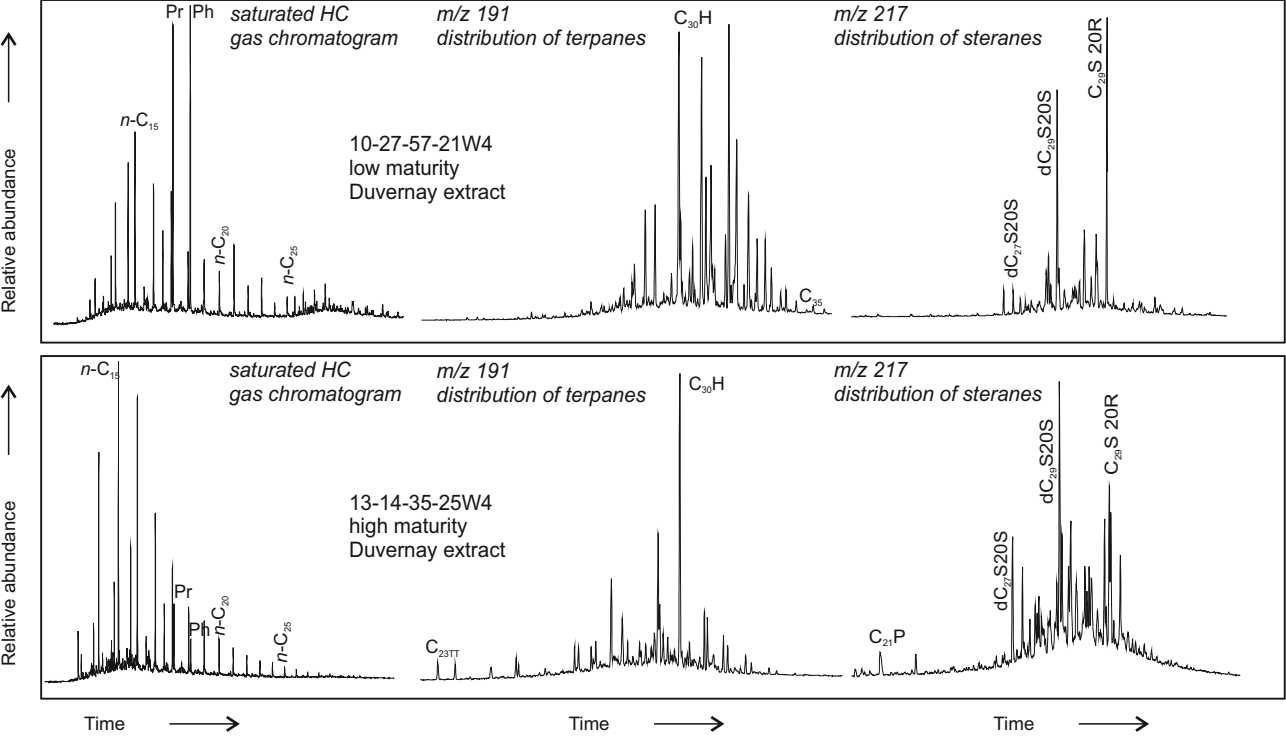
saturated HC
gas chromatogram
m/z 191
distribution of terpanes
m/z 217
distribution of steranes
Pr
Ph
n-C15
n-C20
n-C25
C30H
C35
dC27S20S
dC29S20S
C29S 20R
10-27-57-21W4
low maturity
Duvernay extract
Relative abundance
Time

saturated HC
gas chromatogram
m/z 191
distribution of terpanes
m/z 217
distribution of steranes
n-C15
Pr
Ph
n-C20
n-C25
C30H
C23TT
C21P
dC27S20S
dC29S20S
C29S 20R
13-14-35-25W4
high maturity
Duvernay extract
Relative abundance
Time

Figure 12

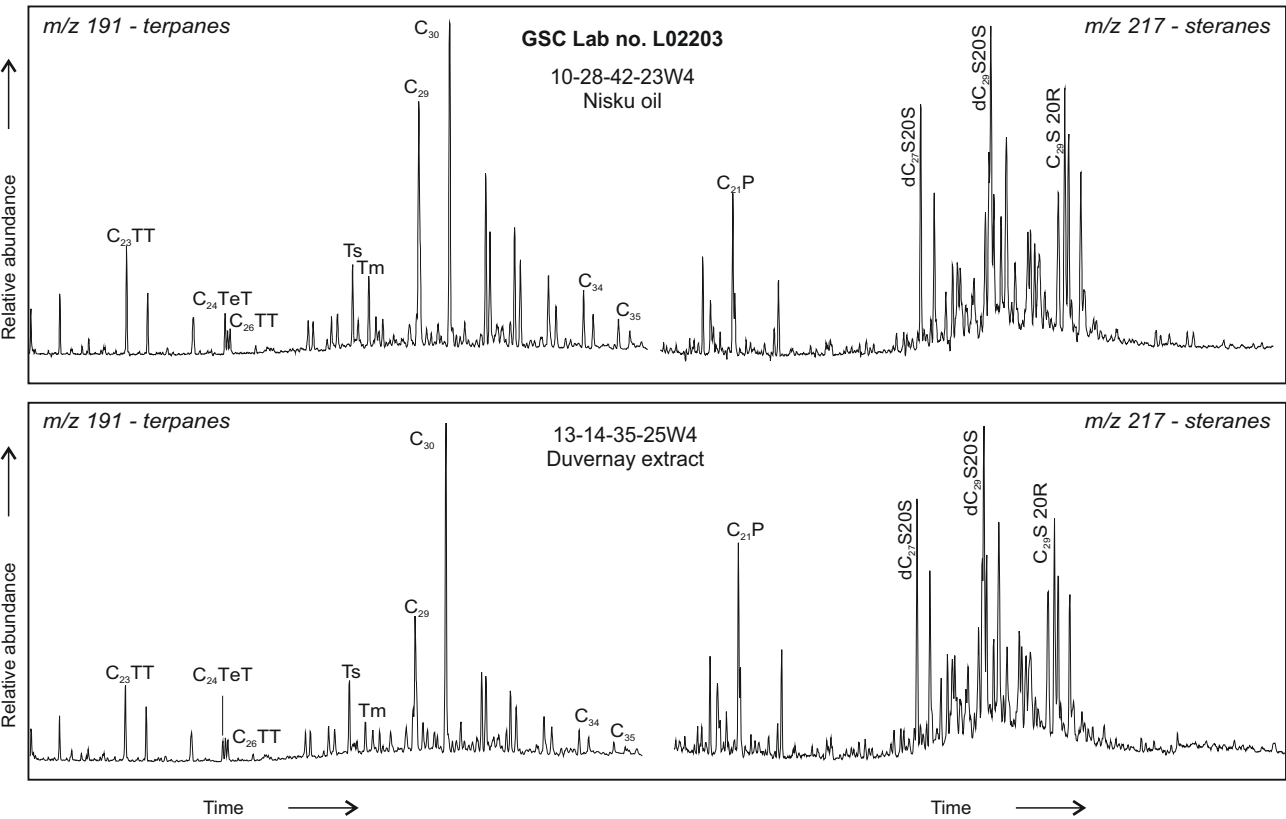
m/z 191 - terpanes
GSC Lab no. L02203
10-28-42-23W4
Nisku oil
m/z 217 - steranes
Relative abundance
C23TT
C24TeT
C26TT
Ts
Tm
C29
C30
C34
C35
C21P
dC27S20S
dC29S20S
C29S 20R

m/z 191 - terpanes
13-14-35-25W4
Duvernay extract
m/z 217 - steranes
Relative abundance
C23TT
C24TeT
C26TT
Ts
Tm
C29
C30
C34
C35
C21P
dC27S20S
dC29S20S
C29S 20R
Time
Time

Figure 13

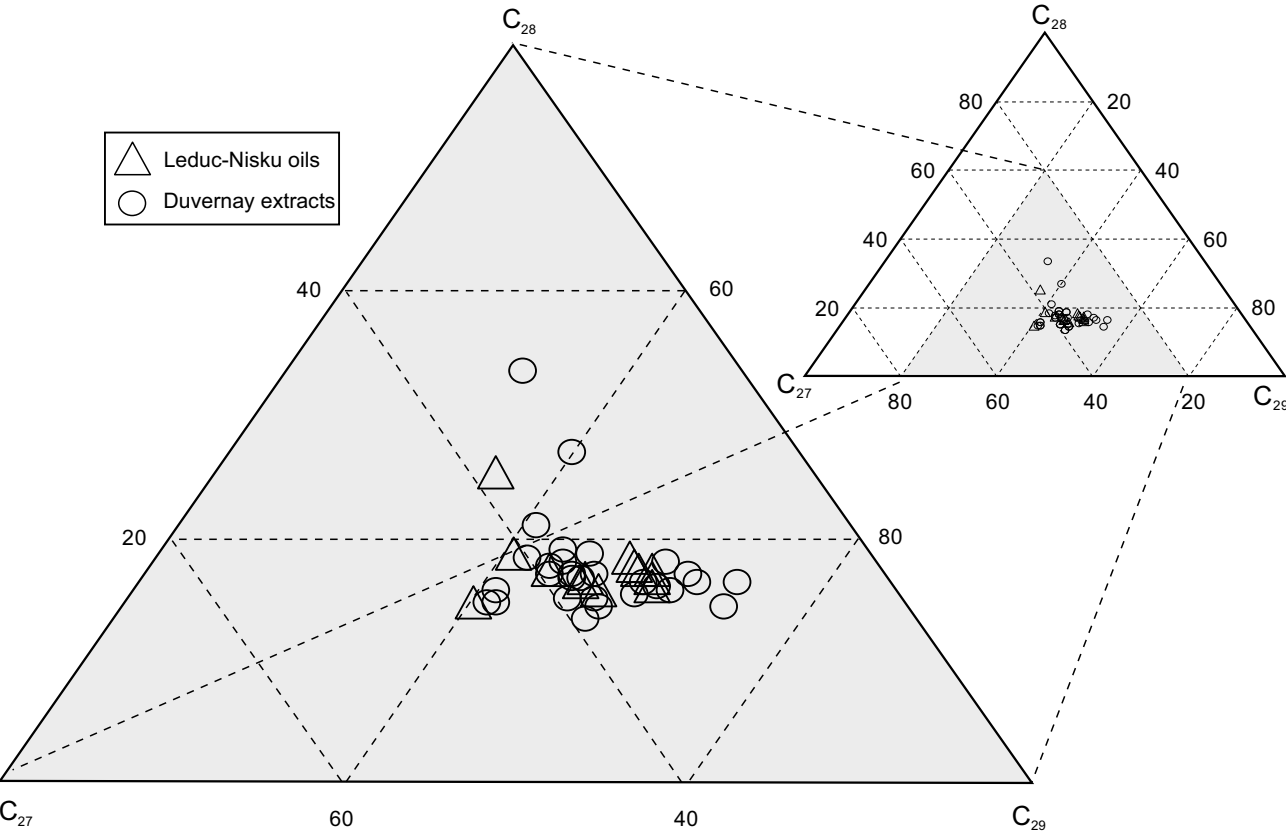
C28
Leduc-Nisku oils
Duvernay extracts
40
60
20
80
C27
60
40
C29
C28
80
20
60
40
40
60
20
80
C27
80
60
40
20
C29

Figure 14

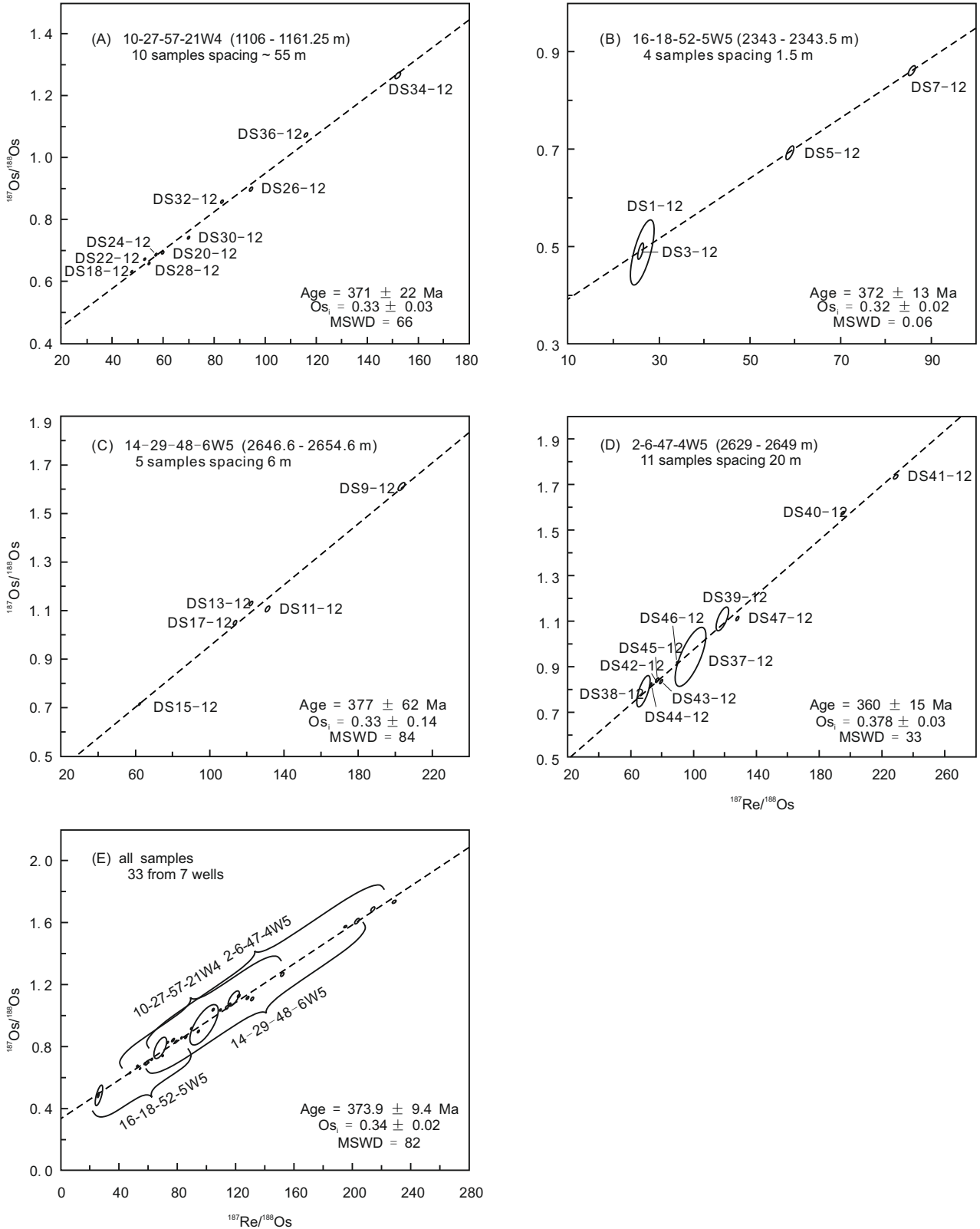
(A) 10-27-57-21W4 (1106 - 1161.25 m)
10 samples spacing ~ 55 m
DS34-12
DS36-12
DS32-12
DS26-12
DS30-12
DS24-12
DS22-12
DS20-12
DS18-12
DS28-12
Age = 371 ± 22 Ma
Os$_i$ = 0.33 ± 0.03
MSWD = 66
(B) 16-18-52-5W5 (2343 - 2343.5 m)
4 samples spacing 1.5 m
DS7-12
DS5-12
DS1-12
DS3-12
Age = 372 ± 13 Ma
Os$_i$ = 0.32 ± 0.02
MSWD = 0.06
(C) 14-29-48-6W5 (2646.6 - 2654.6 m)
5 samples spacing 6 m
DS9-12
DS13-12
DS11-12
DS17-12
DS15-12
Age = 377 ± 62 Ma
Os$_i$ = 0.33 ± 0.14
MSWD = 84
(D) 2-6-47-4W5 (2629 - 2649 m)
11 samples spacing 20 m
DS41-12
DS40-12
DS39-12
DS46-12
DS47-12
DS45-12
DS42-12
DS37-12
DS38-12
DS43-12
DS44-12
Age = 360 ± 15 Ma
Os$_i$ = 0.378 ± 0.03
MSWD = 33
^{187}Re/^{188}Os
(E) all samples
33 from 7 wells
10-27-57-21W4
2-6-47-4W5
14-29-48-6W5
16-18-52-5W5
Age = 373.9 ± 9.4 Ma
Os$_i$ = 0.34 ± 0.02
MSWD = 82
^{187}Re/^{188}Os
^{187}Os/^{188}Os

Figure 15

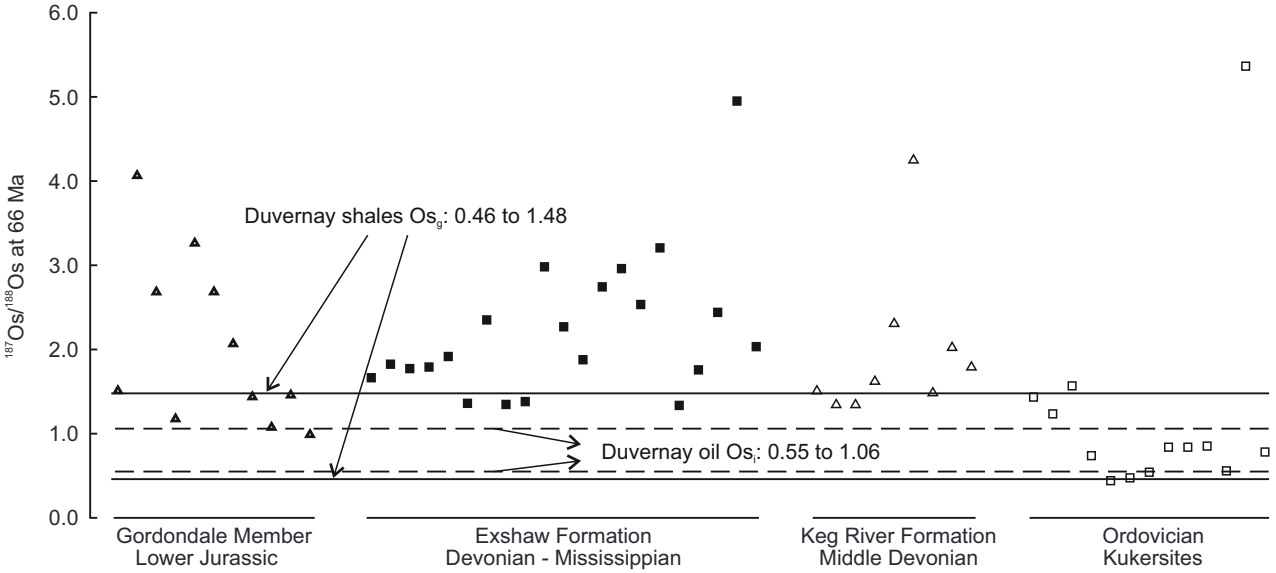
6.0
5.0
4.0
3.0
2.0
1.0
0.0
$^{187}Os/^{188}Os$ at 66 Ma
Duvernay shales Os_g: 0.46 to 1.48
Duvernay oil Os_i: 0.55 to 1.06
Gordondale Member
Lower Jurassic
Exshaw Formation
Devonian - Mississippian
Keg River Formation
Middle Devonian
Ordovician
Kukersites

Figure 16